University of Genoa

Oncolytic immunovirotherapy as an agnostic vaccination against glioblastoma

PhD thesis in

Translational Medicine Biotechnologies

Curriculum: Cellular and Molecular Biotechnologies

XXXV cycle

Supervisor:

Prof. Paolo Malatesta

Candidate:

Francesca Piaggio

Index

Index 2

Abstract 4

1 Introduction 5

1.1 Classification of Gliomas, Glioneuronal tumors and Neuronal tumors 5

1.1.1 High Grade Glioma (HGG) 8

1.2 Standard of care therapies for HGG 9

1.2.1 Surgery 9

1.2.2 Radiotherapy 10

1.2.3 Chemotherapy 10

1.2.4 Tumor-treating fields (TTFs) 11

1.3 Next generation therapies for HGG 11

1.3.1 Immunotherapy 11

1.3.2 Oncolytic viruses 16

2 Previous studies of the research group 22

2.1 HGG murine model 22

2.2 HSV-1 oncolytic virus R-LM113 23

2.2.1 R-LM113 in vitro 23

2.2.2 R-LM113 in mHGG^{pdgf} mouse model 23

2.3 HSV-1 oncolytic virus R-115 24

2.3.1 R-115 in vitro 24

2.3.2 R-115 in mHGG^{pdgf} mouse model 24

3 Rationale 26

4 Results 1: R-115 as a potential therapy for glioblastoma 27

4.1 R-115 efficacy is similar in mHGG^{pdgf}-hHER2- and mHGG^{pdgf}-MIX tumor-bearing mice 27

4.2 Evaluation of R-115 multiple treatment schedules 29

4.3 Characterization of the immune component of long-survivors 30

4.3.1 Splenocytes proliferation 31

4.3.2 ELISpot analysis of IFNγ released by splenocytes 31

4.3.3 Release of Granzyme B as cytotoxicity marker 32
4.4 Characterization of the effects induced by the immune system on tumor cells 33
4.4.1 LS splenocytes mediated tumor cells death 33
4.4.2 LS splenocytes restore MHC-I expression on tumor cells 34
5 Results 2: Splenocytes ex vivo stimulation and training against mHGG^{pdgf} cells 35
5.1 Setting up of activating culturing conditions 35
5.2 Activated splenocytes enhance tumor cells death of oHSV-infected tumor cells 35
5.3 MHC-I recovery on tumor cells 35
5.4 Splenocytes from LS increase survival of mHGG^{pdgf} bearing mice 37
6 Methods 38
6.1 R-LM113 38
6.2 R-115 38
6.3 Animal procedures - Murine model of mHGG^{pdgf} 38
6.4 Cell culture 39
6.5 Flow cytometry 40
6.6 ELISA 40
6.7 ELISpot 41
6.8 Luciferase assay 41
6.9 Statistical analysis 41
7 Discussion 42
8 Conclusion 44

Abstract

High grade gliomas (HGG) are aggressive tumors characterized by high heterogeneity, immune modulated environment and resiliency to standard treatments. Despite the HGG frequency is about 5 people every 100000, the overall survival (OS) rate at one year is extremely low. Standard of care treatments are invasive and never resolving while alternative approaches like immunotherapy and oncolytic virotherapy are showing promising outcomes. In this thesis are discussed the results obtained by the employment of an innovative therapy based on the combination of immunotherapy and oncolytic virotherapy. A new oncolytic HSV, R-115, has been evaluated for its ability to increase survival and rescue immunocompetent mice previously injected with murine HGG. The effects of R-115 immunovirotherapy were tested in two murine models, based on completely or partially targetable cells, respectively. The analyses were also focused on the ability of R-115 treatment to induce an immune memory which prevented secondary transplanted tumors and prolonged survival when administered as cell therapy. Altogether, our investigations candidate R-115 as a valuable alternative to common treatments and encourage further investigation to evaluate its potential for clinical application.

1 Introduction

1.1 Classification of Gliomas, Glioneuronal tumors and Neuronal tumors

Gliomas are the most common primary tumors of the central nervous system. Brain tumor research in the last few decades has clearly shown that the knowledge of the tumor molecular characteristics can be more effective than a traditional histogenetic assessment based on immunohistochemistry and electron microscopy. Despite it is important to prioritize molecular information over histopathological characteristics, it is the integrated assessment of all the available information that leads to the final diagnosis. The importance of DNA methylation profiling was underlined by its ability to identify 22 newly recognized tumor types. Still, given the general inaccessibility of the test, methylome profiling as a primary routine diagnostic method is not recommended yet [1].
In 2021 the WHO published the 5th edition of the classification of tumors of the central nervous system which introduces some major changes and distinguished 6 major groups of gliomas (Figure 1).

Figure 1. Six major categories of gliomas, according to WHO 2021 5th classification.

Fourteen newly recognized types have been added to the classification of Gliomas, Glioneuronal tumors and Neuronal tumors and, for some of these, integrating histological appearance and molecular features are required to reach diagnosis. To be noted that adult-type and pediatric-type are primarily adult and pediatric tumor respectively, but, sometimes, pediatric-type can occur in adult and, more rarely, adult-type can occur in children [2].
In particular, the new classification revisits Gliomas, Glioneuronal tumors and Neuronal tumors dividing them into six categories:

I. Adult-type diffuse gliomas:

- Astrocytoma, IDH (Isocitrate Dehydrogenase (NADP(+))-mutant. Can be graded as CNS WHO grade 2, 3 or 4 (grading is no longer entirely histological. CDKN2A/B homozygous deletion results in a grade 4, even in the absence of microvascular proliferation or necrosis).
- Oligodendroglioma, IDH-mutant and 1p/19q-codeleted

- Glioblastoma, IDH-wildtype. Diagnosed by the presence of 1 or more genetic parameters like TERT promoter mutation, EGFR gene amplification, combined gain of the entire chromosome 7 and loss of entire chromosome 10 [+7/-10] or microvascular proliferation or necrosis.

II. Pediatric-type diffuse low-grade gliomas (expected to have good prognosis). These tumors feature diffuse growth in the brain but with sometimes overlapping and less specific histological characteristics:

- Diffuse astrocytoma, MYB- or MYBL-1-alterated
- Angiocentric glioma
- Polymorphous low-grade neuroepithelial tumor of the young (PLNTY)
- Diffuse low-grade glioma, MAPK pathway altered

III. Pediatric-type diffuse high-grade gliomas (expected to be aggressive). Except for the diffuse midline glioma, the other three are newly added:

- Diffuse midline glioma, H3 K27-altered
- Diffuse hemispheric glioma, H3 G34-mutant
- Diffuse pediatric-type high-grade glioma, H3-wildtype and IDH-wildtype
- Infant-type hemispheric glioma. Occurs in newborns and infants with a distinct molecular profile with fusion genes involving ALK, ROS1, NTRK1/2/3 or MET.

IV. Circumscribed astrocytic gliomas (where circumscribed is intended as not diffuse):

- Pilocytic astrocytoma
- High-grade astrocytoma with piloid features
- Pleomorphic xanthoastrocytoma
- Chordoid glioma
- Astroblastoma, MN1-altered

V. Glioneuronal and neuronal tumors (different tumors united by neurological differentiation). Three new types have been added:

- Ganglioglioma
- Desmoplastic infantile ganglioglioma/desmoplastic infantile astrocytoma
- Dysembryoplastic neuroepithelial tumor
- Diffuse glioneuronal tumor with oligodendroglioma-like features and nuclear clusters (DGONC, provisional)
- Papillary glioneuronal tumor
- Myxoid glioneuronal tumor
- Diffuse leptomeningeal glioneuronal tumor
- Gangliocytoma

- Multinodular and vacuolating neuronal tumor
- Dysplastic cerebellar gangliocytoma (Lhermitte-Duclos disease)
- Central neurocytoma
- Extraventricular neurocytoma
- Cerebellar liponeurocytoma

VI. Ependymomas (classified by site, histological and molecular features):

- Supratentorial ependymoma
  - Supratentorial ependymoma ZFTA fusion
  - Supratentorial ependymoma YAP1 fusion
- Posterior fossa (PF) ependymoma
- Posterior fossa (PF) ependymoma, group PFA
- Posterior fossa (PF) ependymoma, group PFB
- Spinal ependymoma
- Spinal ependymoma, MYCN amplified
- Myxopapillary ependymoma
- Subependymoma

1.1.1 High Grade Glioma (HGG)

According to the 2021 classification, high grade gliomas (HGG) that previously were referred to Glioblastoma IDH-mutant and -wildtype, are now Astrocytoma IDH-mutant and Glioblastoma IDH-wildtype. High grade gliomas (stage IV) are now considered also diffuse Astrocytoma, IDH-mutant with ATRX loss, P53 mutation and CDKN2A/B deletion and diffuse Astrocytoma, IDH-wildtype with gain of chr7/loss chr10, EGFR amplification and TERT promoter mutation (Figure 2A-B) [1], [3].

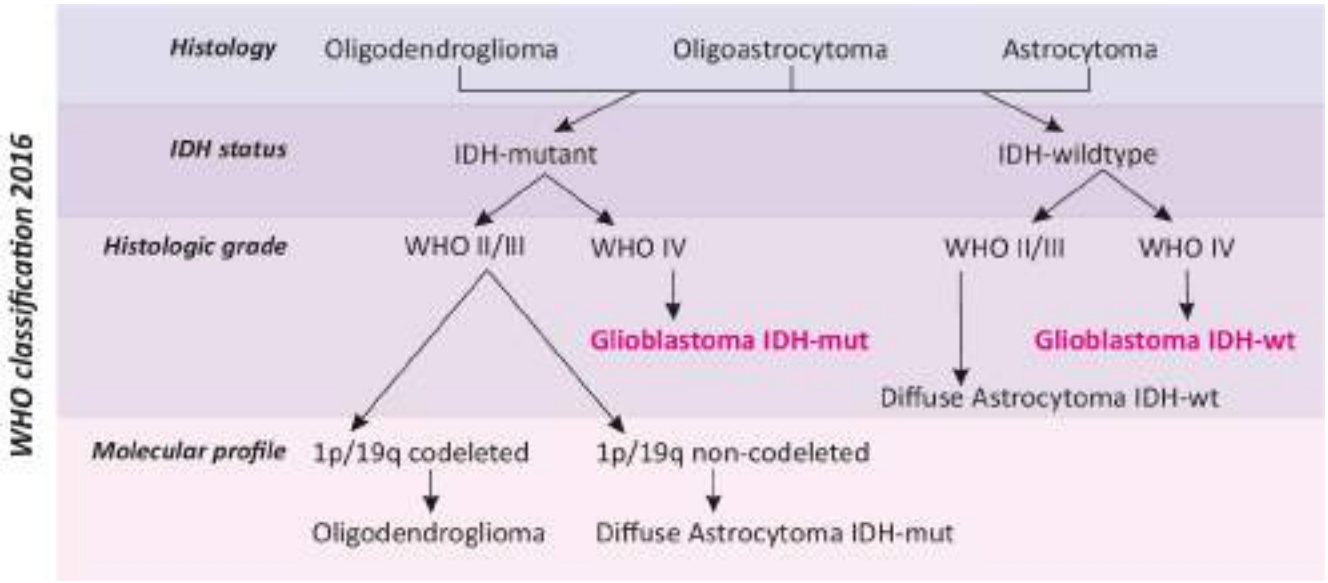

Figure 2A. Schematical representation of WHO 2016 adapted from Gritsch et al. 2022.

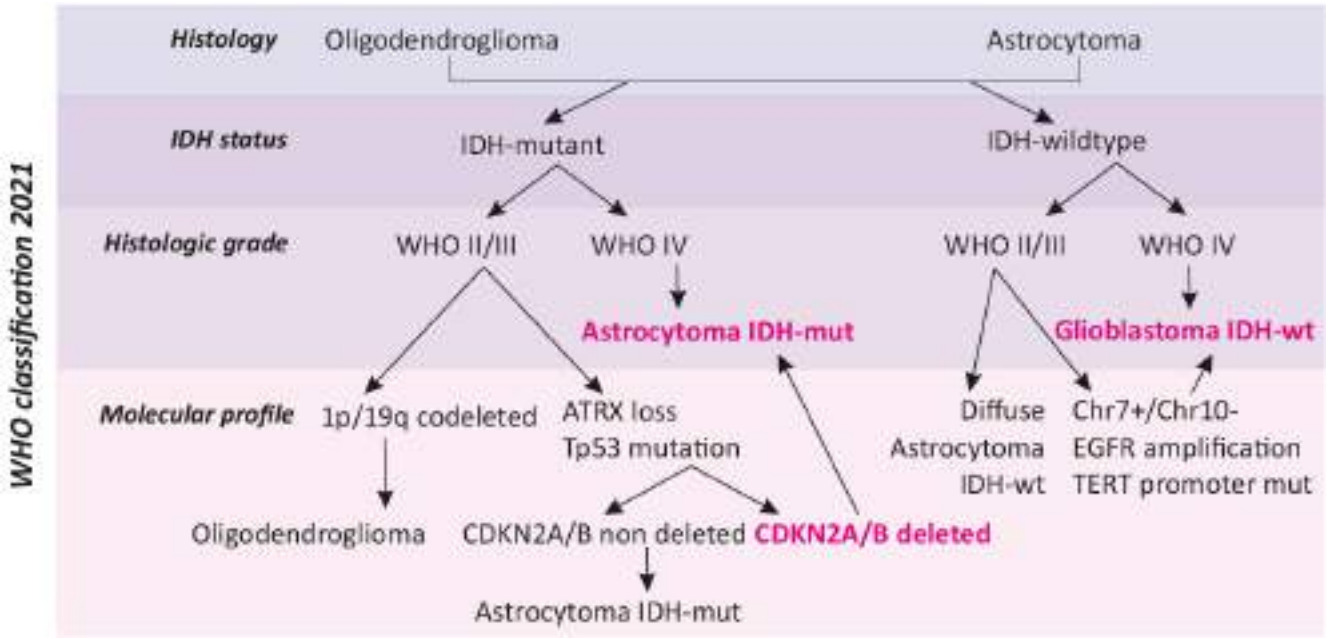

Figure 2B. Schematical representation of WHO 2021 classifications adapted from Gritsch et al. 2022.

Since the new classification of the tumors of the central nervous system is particularly recent, almost all the literature about brain tumors refers to the previous 2016 classification.
Glioblastoma is the most common and the most aggressive tumor of the central nervous system. Up to 15% of all primary brain tumors and 45% of malignant primary brain tumors are glioblastomas [4]. The incidence rate can vary between different countries or even regions and in 2015 was about 4.32 in US, 4.5 in Canada and 5.02 per 100,000 in England with an increasing trend if compared to the ten previous years [5]. Median age at diagnosis is 65 years and it is approximately 1.6 times more common in males than females [6].
The 5-year survival rate of glioblastoma patients is approximately 5.5% in the US and the median overall survival (OS) is about 1 year. The median OS relates to surgical treatment: it goes from 15.5 month in case of gross total resection to 11.7 months for subtotal resection to 5.6 months without resection [7]. Differences can also depend on the considerable heterogeneity in the anatomic distribution of HGG within the brain. More than 40% are located in the frontal lobe, around 30% in the temporal, 25% in the parietal and 3% in the occipital lobe [8].
Even if high grade gliomas are more frequent in adult than children [9], pediatric CNS tumors are the second most common childhood malignancy and the most frequent solid tumor resulting in the main cause of death among all childhood cancer. Younger children have higher incidence of tumors of embryonal origin while older patients have more often tumors of glial origin. Of all childhood gliomas, 20% are HGGs and occurs with an incidence of 0.8 per 100,000 children per year. Children with HGGs have an overall poor prognosis despite intensive therapy [10].

1.2 Standard of care therapies for HGG

Standard treatment includes maximal safe resection followed by concomitant radiotherapy and temozolomide (TZM) chemotherapy and then adjuvant TZM. Key supportive medications may include corticosteroids for vasogenic edema and anti-epileptic medication, in case of seizures [11].
The extent of surgical resection remains one of the most important prognostic factors in predicting outcome. Together with surgery, the main therapy is based on local site radiation of 5000 to 6000 cGy while the benefits of chemotherapy as well as other adjuvant therapy remain controversial [10].

1.2.1 Surgery

Even before Stupp protocol (Temozolomide combined with radiotherapy), surgery was the main first line treatment. The primary goal is to achieve a gross total resection (GTR) as precisely as possible in order to prevent any damage to the patient's functional state. Full resection is associated with higher chance of survival. To ameliorate surgery and minimize collateral effects, many surgical approaches have been improved. These tools include surgical navigation with functional MRI (fMRI), functional monitoring and fluorescence-based visualization of tumor tissue with 5-aminolevulinic acid (5-ALA) or fluorescein.

Fluorescein, administered intravenously 3-20mg/kg, was the first agent to be utilized intraoperatively. Due to the extra time between injection and resection, it is retained only by regions where the blood brain barrier is damaged [12].
Another possible agent is 5-ALA, selectively uptaken by glioblastoma, administered 20mg/kg by oral solution and converted into protoporphyrin IX (PPIX). Nowadays, almost all surgical microscopes can benefit from PPIX visualization [13].
When tumor invade eloquent areas, brain mapping in awake patients, evoked potentials or electromyography have shown beneficial results in terms of neurological functions. Awake craniectomy (AC) performed with intraoperative electrodes for motor and speech monitoring returned remarkable results [14]. For this reason, it is the gold standard in case of diffuse brain tumor. Intraoperative magnetic resonance imaging (I-MRI) has also been associated to awake craniectomy. It is based on real-time intraoperative MRI imaging that detects tumor and its residues [15].

1.2.2 Radiotherapy (RT)

The standard of care (SOC) protocol dosage is 50-60 Gy in 1.8-2-0 Gy daily portion over 6 weeks. Other radiotherapy doses, schemes and ionizing radiation techniques have been tested for primary glioblastoma but no remarkable results were obtained. RT can also be adjusted according to Karnowski performance scale index. Adaptive RT is emerging as the possibility to start with a dosage and then evaluate the following treatments according to the effects obtained after the first one [16].
After the first RT course, radio-resistance can occur. This could be partially explained by the considerable increase of hyaluronic acid (HA) after RT which, interacting with CD44 receptor, can induce mesenchymal shift in GBM cells [17].
Different ionizing radiation treatments are still under investigation such as intensity-modulated RT, proton or heavy ion irradiation, stereotactic radiotherapy (SRT), radiosurgery (SRS) and hypo- and hyper-fractioned regimens. Various combination, including drugs like bevacizumab seems also promising [16].

1.2.3 Chemotherapy

Temozolomide is an oral drug capable to penetrate the blood brain barrier. After entering into the cytoplasm, TZM undergoes spontaneous hydrolysis to form monomethyl triazene 5-(3-methyltriazene-1-yl)-imidazole-4-carboxamide (MTIC) which is then hydrolyzed to form the methyldiazonium. This compound adds a methyl group to purines and pyrimidines in DNA resulting in cell damage, apoptosis and cell cycle arrest. Only patients who have methylated MGMT, an enzyme involved in DNA repair, can benefit from TZM treatment. Thus, when MGMT is activated, it counteracts TZM effect. Sadly, only about 45% of patients have a methylated MGMT [18]. The most common side effects of alkylating agents are myelosuppression, especially thrombocytopenia, neutropenia, nausea and hepatic damage. Considering its impact in the treatment with TZM, the evaluation of MGMT methylation status is important in primary management of glioblastoma patients.

Alternatives to TZM are other alkylating agents such as lomustine, carmustine and nomustine. These nitrosoureas alkylate DNA and RNA as well as crosslink DNA, acting also when the cells are not actively dividing. Lomustine acts also by carboxylating amino acids, impeding enzymatic processes and leading to cells death [19].

1.2.4 Tumor-treating fields (TTFs)

Tumor-treating fields are recently approved treatments that use transducer arrays applied directly to the scalp to give low intensity (1-3V/cm), intermediate-frequency (200 Hz) alternating electric fields. TTFs is applied both for newly diagnosed and, most importantly, recurring glioblastoma. TTFs generate selective toxicity in quickly dividing cells. Despite evidence showed the potential benefits of TTFs, this technique is still debated because of the high costs and the poor accessibility [20].

1.3 Next generation therapies for HGG

1.3.1 Immunotherapy

A completely different methodology for the treatment of HGG is based on immunotherapy that, with different approaches, induces an antitumor activity where the immune system is the key player.
The importance of the therapeutic role of the immune system for cancer treatment was first highlighted by Doctor William Coley who is considered the father of immunotherapy. After noticing that patients diagnosed with sarcoma and affected by Streptococcus pyogenes went into spontaneous long-term remission, in 1891 he treated patients with Coley's mixed toxin achieving up to complete remission for patients with various malignancies. Despite at that time the mechanisms involved were not clear, nowadays the importance of a proper stimulation of the immune system against cancer cells is well known. In 1909 Paul Ehrlich hypothesized that tumors may be controlled by the immune system and in 1957 Thomas and Burnet proposed the theory of cancer immunosurveillance, suggesting that lymphocytes could act as guards responsible for the elimination of mutated cells, theory confirmed by the incidence of cancer in patients with immune suppression related disease [21]. The interaction between the immune system and cancer cells is not always beneficial for patients since tumors are imprinted by the immunologic environment in which they form. This continuous interacting process can consequently generate tumors that are more able to resist to tumor suppressing action.

1.3.1.1 Elimination, Equilibrium and Escape

The host-protecting and tumor-sculpturing dual action of the immune system is better described by the three phases of the immunoediting (Figure 3).

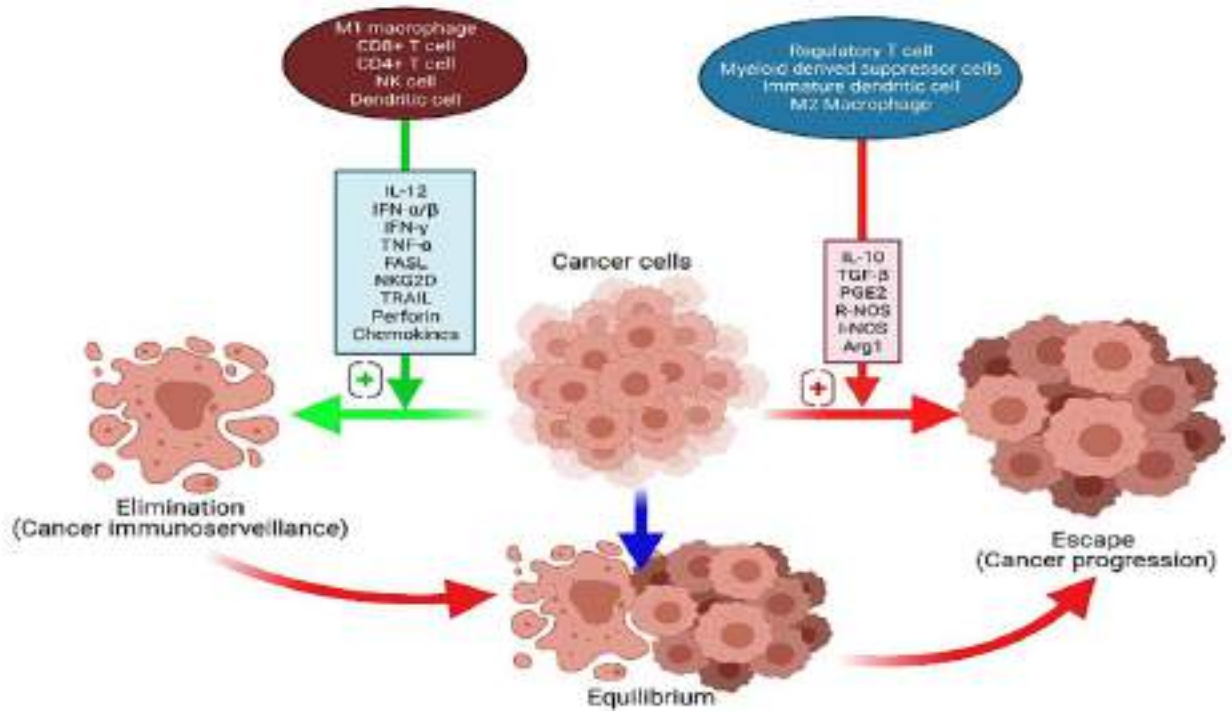

Figure 3. Schematic representation of the immune system balancing between anti-tumoral and pro-tumoral activity (Mallick et al. 2021).

The three phases consist in:

- Elimination: in this phase the immunosurveillance takes place. When solid tumors reach a certain size, they need more blood supply obtained by production of stromagenic and angiogenic proteins. Inflammatory signals are induced and cells of the innate immune system are recruited. Infiltrating cells like NKT, NK and γδT recognize transformed cells and release IFNγ. Secondly, IFNγ can induce the production of chemokines from the tumor and normal host cells which can have a potent angiostatic capacity thus blocking the formation of new vessels. Chemokines recruit NK and macrophages which transactivate one another producing IFNγ and IL-12. In the end, specific CD4 and CD8 T cells destroy the remaining antigen-bearing tumor cells.

- Equilibrium: if the elimination process is unsuccessful, there is progression. The equilibrium phase leads to a Darwinian selection of tumor variants. Different mutation can bring to new variants with increased resistance to immune attack. This phase is likely to be the longest and could take even years.

- Escape: immune-resistant variant are no longer hittable by the immune system, begin to expand in an uncontrolled manner, resulting in a malignant disease [22].

1.3.1.2 Hot tumors and cold tumors

It is well known by now that cancer progression is not only mediated by genetic alterations within tumor cells but also that the surrounding niche has a critical role. Virchow was the first to suggest a possible connection between chronic inflammation and tumorigenesis. About 15% of global cancer burden is attributable to infectious agents and inflammation is a major component of these chronic infections [23]. Given its contradictory role, the tumor microenvironment (TME) gained increased attention. Differently from liquid tumors, solid tumors are surrounded by many cellular (vascular endothelial cells, fibroblasts, immune cells) or extracellular components like extracellular matrix and soluble molecules (i.e. cytokines, chemotactic factors, growth factors). The importance of TME was highlighted by the failing of multiple approaches based on direct targeting of tumor cells and by different response obtained by patients with the same kind of cancer but different immune cell composition within the TME.

Tumors can be divided into two categories according to the responsive state of their immune component: hot tumors, characterized by an active antitumor response mediated by T lymphocytes infiltration and cold tumors, characterized by the absence or exclusion of T cells in the tumor parenchyma. Many components can influence the status of a TME [24]. Abundant infiltration of CD3+ and CD8 T cells has been associated as a marker of immune recognition but T cells need to be localized near the tumor cells [25]. Higher ratio of Th1/Th2 is also associated with stronger antitumor immune response [26]. Treg has been shown to be co-recruited with CD8 T cells, preventing them from accessing the tumor. CD8 Treg have also been reported as cells capable to suppress immune activation. According to these findings, the hotness of a tumor should consider the different ratio and subtype of T cells instead of the abundance in the TME [27].

NK cells are another important component of the TME. They can express both Programmed Cell Death 1 (PD-1) and its ligand (PD-L1) and, therefore, an abundant NK infiltrate could induce a better response in tumor treated with immune checkpoint inhibitors (ICI). Also, NK affect the adaptive immune response by inducing DC maturation via cytokine secretion [28].

Tumor specific antigens (TSAs) are the main elicitors of T cell-mediated immune response. Neoantigens can originate from nonsynonymous mutations, gene fusion, noncoding region mutations and alternative splicing. Gene mutation can also arise from deficiencies in DNA repair, which is the case of mismatch repair deficiency (dMMR) and subsequent microsatellite instability (MSI). The abundance of neoantigens is associated with a high tumor mutational burden (TMB), definable as the number of mutation per megabase (Mut/Mb) of DNA sequenced in a specific cancer. The more are the TSAs the more recognizable is the tumor [29].

HLA-I molecules are other important players for the immunosurveillance that can be genetically, epigenetically and transcriptionally downregulated by tumor cells.

The role of presenting antigens via MHC molecules is mediated by antigen presenting cells (APCs), mostly DCs which are responsible of the activation of NAIVE T cells. APC are recruited by chemokines and activated by danger signals as a consequence of immunogenic cell death of tumor cells. The released signals can be pathogen-associated molecular patterns (PAMPs) such as cytosolic DNA and

RNA and damage-associated molecular patterns (DAMPs) such as mtDNA, ATP and some cytokines released. DC can be dysfunctional for different aspects, including recruitment, activation, maturation, antigen cross-presentation or priming [27].
All these studies about the TME underline that, even in the presence of a high TMB and a strong infiltrate, tumor can immune escape acting through many different mechanisms like the remodeling of CD8 lymphocytes, secretion of proinflammatory cytokines and reducing antigen presentation.

1.3.1.3 Existing immunotherapies

The key outcome of immunotherapy is the proper activation of the immune system without major off target effects like the induction of autoimmune responses or cytokine release syndrome.
Immunotherapy can be active, with the development of immune memory and long-lasting response, or passive, requiring regular drugs administration.
The main categories of immunotherapies are [30]:

- Cancer vaccines: based on the immunization against tumor specific antigens. DC are the best equipped APCs. DC-based vaccines involve the reinfusion of DC previously pulsed with tumor antigens or tumor cell lysates and stimulated with a defined maturation cocktail ex vivo [31]. Immune responses can also be induced by whole tumor cells. This is the case of GVAX, a cancer vaccine composed by autologous tumor cell genetically modified to secrete GM-CSF [32].

- Cytokine therapy: as a response to different cellular stress like infection, inflammation and tumorigenesis, cytokines can be released both by immune and nonimmune cells. A large administration of IL-2, which has the ability to expand T cells, could lead to cancer regression [33]. Another example is the interferon α (IFNα), a pleiotropic cytokine which plays a critical role on the antitumor immunity. TNFα induce senescence, apoptosis and stimulates DC maturation and the enhancement of T-cell toxicity [34]. Despite the theoretical employment of cytokines should be successful, the strong and uncontrolled stimulation can lead to severe toxic effects and poor tolerability.

- Adoptive cell transfer (ATC): utilize autologous immune cells isolated or genetically engineered, expanded ex vivo and reinfused as therapy. The two main type of engineered cells are chimeric antigen receptor (CAR)-T cells, modified to express antibody fragments capable to recognize antigens expressed by cancer cells and T cell receptor (TCR)-engineered T cells, modified to express tumor antigen specific receptor α and beta chains that are originated from high-quality and high-avidity antigen-specific T cell clones [35].

- Immune checkpoint inhibitors: immune checkpoints are molecules of coinhibitory signaling pathways that act to maintain immune tolerance but can be exploited by cancer cells to escape immunosurveillance. The main checkpoints are cytotoxic T lymphocyte-associated antigen-4 (CTLA-4) and programmed cell death-1 (PD-1) which are expressed on T cells and negatively regulates T cells activation and immune response, respectively and the ligand of PD-1 (PD-L1), which is commonly

expressed by normal tissues to regulate immune tolerance. NK cells express both PD-1 and PD-L1. PD-L1 can also be abnormally expressed by tumor cells to escape immune surveillance by suppressing the proliferation and cytokines secretion in PD-1 expressing T cells [36].

Blocking immune checkpoint with inhibitors (ICI) can prevent the negative signaling induced by their activation. Blocking CTLA-4 with antibodies induced effective immune responses and tumor regression. Ipilimumab, a monoclonal antibody blocking CTLA-4, became the first ICI approved for cancer treatment [37]. The first antibody approved targeting PD-1 was nivolumab followed by pembrolizumab. Many anti-PD-L1 antibody, like atezoliumab, avelumab and durvalumab showed positive responses in a variety of malignancies. Still, antibody-based drugs have some disadvantages such as immunogenicity issues and poor permeability in tumor tissues [38].

1.3.1.4 Immunotherapy for HGG

Bevacizumab (BEV) is the most investigated immunotherapeutic drug. It is a humanized monoclonal antibody against VEGFR which is overexpressed in glioblastoma. BEV has been evaluated alone, in combinations with Lomustine or irradiation (+/- TZM) [39]. The results obtained are controversial but this drug still obtained FDA approval for recurrent glioblastoma in several countries, including US but not Europe. Among the previously described immunotherapies, like immune check point inhibitors, many have been tested also for high-grade gliomas. Indeed PD-L1 was observed in 61-88% of patients but is not the presence that is indicative rather the expression level [40]. Some monoclonal antibodies targeting PD-1 (nivolumab, pembrolizumab and cemiplimab) and targeting PD-L1 (durvalumab, avelumab and atezolizumab) have been investigated. The effect of ipilimumab, targeting CTLA-4, was also evaluated. Together with these surface molecules, other targets of checkpoint inhibitors are under investigation, like CD47, CD24, CD37, LAG-3 and TIGIT/CD96 [41].

Other tested strategies include CAR-T and CAR-NK. Example of CART targets are IL13-Rα2, HER2 and EGFRvIII. Unfortunately, limitations occur due to the high heterogeneity of glioblastoma. These limitations are partially overcome with last fourth generation engineered lymphocytes which include more stimulatory domains and additional proteins.

Finally, other immunotherapeutic approaches evaluated are based on vaccine therapy. There are three main approaches in vaccine therapy based on tumor-specific antigens, cell-based therapies and viral vector vaccines transporting tumor antigens as mRNA. One of the main targets on glioblastoma is EGFRvIII, a mutation of the Epidermal Growth Factor Receptor (EGFR). EGFRvIII, which is expressed in about 20-30% of glioblastoma, causes constitutive activation, resulting in augmented proliferation. Rindopepimut was the first developed vaccine specific for EGFRvIII but, despite the initial encouraging results, it was subsequently suspended due to lack of benefits [42].

Vaccine have been developed also with DCs. ICT-107 is a vaccine based on autologous DCs targeting 6 tumoral antigens (HER2, TRP-2, MAGE-1, gp100, AIM-2 and ILR αa2) but results were slightly improving. Another DC-based vaccine is DCVax-L but results are controversial. Other trials proved the safety of DC vaccines but the OS was not improved.

Vaccines were also developed with up to 20 personalized neoantigens (NeoVax) extracted from patient's resected tumor. NeoVax in combination with ICI is under investigation [43].

1.3.2 Oncolytic viruses

Oncolytic virotherapy is based on the employment of viruses specifically selected for their natural or engineered ability to infect and kill cancer cells.

As for many others breakthrough in science, the employment of oncolytic viruses (OVs) started from empirical observations. It was noticed that a number of cancer patients went into short periods of clinical remission when they contracted an infectious disease [44]. Most of the time, patients were affected by hematological diseases associated with suppression of the immune system like leukemia, Hodgkin's disease and Burkitt's lymphoma [45], [46]. The reason of the therapeutic potential associated with viral infection is the ability of some viruses to damage preferentially tumor tissues than healthy ones and to stimulate the immune system as a consequence of the infection.

After observing that virus infection could ameliorate conditions of oncologic patients, first generation oncolytic viruses were employed in one of the first clinical trial in 1949 by Hoster and colleagues. They treated 21 patients affected by Hodgkin's disease with a total of 35 samples of sera and tissues extracts containing the hepatitis virus, resulting in limited benefits and risk to develop hepatitis [47]. Okuno and colleagues get better results in 1978 when they published their research on Mumps virus for the treatment of different kind of human cancers. They treated 200 cancer patients with purified mumps virus. Patients arose extremely mild side effects but gained astonishing results, including cancer regression in 26 patients [48].

Initially, when direct genetic manipulation was not possible, scientist tried to improve oncolytic or tumor-specific activity by in vitro manipulation. Moore demonstrated that serial passage of an oncolytic virus improves its killing activity [49]. Like that, first generation OVs as wild-type non-engineered in vitro-passaged viruses were born. Since the OVs research kept improving, research came to second generation viruses based on recombinant selectivity-enhanced viruses and subsequently to third generation OVs based on viruses armed with therapeutical genes [50].

Many viruses are constantly engineered to reduce their pathogenicity thus maintaining or increasing the oncolytic activity and improving the tumor specificity [44].

Several viruses have been investigated as potential oncolytic virotherapy. Among DNA viruses there are Herpes simplex virus-1, Human adenovirus, Vaccinia virus and Myxoma virus. Many other RNA viruses have been studied like Mumps virus, Newcastle disease virus, Vescicular stomatitis virus, Reovirus, Measles virus, Poliovirus, Coxsackie virus, Echovirus (type I) and the Influenza virus.

1.3.2.1 Oncolytic therapy for the treatment of HGG

The great potential of oncolytic viruses as cancer therapy has also been deeply investigated for the treatment of glioblastoma. OVs employed against glioblastoma can selectively infect and kill cancer

cell thanks to their selective replication in tumor cells or because they have been modified to target specific receptor like EGFRvIII, PDGFR, IL-13 or RGD peptide.
Examples of viruses developed for glioblastoma treatment are adenovirus (i.e.DNX-2401, Ad5-delta-24-RGD), parvovirus (ParOryx), measles virus (MV-CEA), poliovirus (PVS-RIPO) and replicating retroviral vector (Toca511) which showed safety and efficacy both in preclinical and clinical phase trials. The combination with combined immunotherapy is also under evaluation [51].

1.3.2.2 HSV-1 as strategic oncolytic virus

The deep knowledge and understanding of HSV has allowed the development of potential therapeutic agents and vectors for several applications in human diseases, including oncolytic HSV (oHSV) [50].
HSV-1 and HSV-2 are important human pathogens that cause a variety of diseases including herpes labialis, genital herpes, herpes stromal keratitis (HSK), eczema herpeticum, disseminated disease in the neonate, meningitis and herpes simplex encephalitis (HSE). Several reports suggest also a link between HSV infection and neurodegenerative diseases [52], [53].
The major disadvantage of oHSV is possibly the prior immunity in the human host which can partially counteracted by the route of administration [54]. On the other hand, HSV shows many advantages as oncolytic agent: it has four cellular receptors with a broad host range that allows the virus to infect and replicate in almost all cell lines (property that need an adequate detargeting of the undesired receptors), property that could also protect against the rapid development of resistance to virotherapy; it can infect both replicating and non-replicating cells; it has the potential for incorporating a large size of foreign DNA; the undesired toxicity from the virus replication can be controlled by effective anti-herpetic agents such as acyclovir, ganciclovir, valacyclovir and famciclovir; compared to other virus, lytic infection by HSV usually kills target cells much more rapidly and effectively; it can infect many kinds of animals making HSV preclinical studies easier; can induce strong immunogenicity and cell toxicity that are beneficial when developing vaccine vectors or anticancer agents [50] and finally, it has the ability to synergize with checkpoint blockade, and to confer sensitivity to and widen the activity of checkpoint inhibitors [54].

1.3.2.2.1 HSV-1 mechanism of infection and structure

HSV-1 typically infect epithelial cells and neurons but can also infect other cells, including fibroblasts and lymphocytes. Entry into epithelial cells occurs by low pH-dependent fusion with the endosomal membrane, whereas entry into neurons occurs by fusion at the plasma membrane [53], [55].
Following primary infection, virus gains access to the sensory nerve fibers of the peripheral nervous system (PNS) and is transferred by retrograde microtubule-associated transport to the cell body of the neuron where it establishes latent infection [56].
HSV-1 is a double-stranded linear DNA virus with a genome of 152 kb encoding over 80 distinct genes [57]. The HSV genome consists of two long structures of unique sequences (designated long (UL) and short (US)), both of which are flanked by a pair of inverted repeat regions (TRL–IRL and IRS–TRS).

The viral DNA is contained in a viral icosahedral capsid surrounded by an amorphous layer known as the tegument, which contains viral structural and regulatory proteins, and an external envelope containing numerous glycoproteins. The HSV diameter is about 100 nm [50].
HSV-1 infection is initiated in epithelial cells at mucosal surfaces upon initial binding of viral glycoproteins gB and gC with host cell surface heparan sulfate proteoglycans. This allows attachment of the viral glycoproteins gB, gD, and gL to host cellular receptors such as nectin-1, herpes virus entry mediator (HVEM), or 3-O-sulfated heparan sulfate for membrane fusion and viral entry (Figure 4).

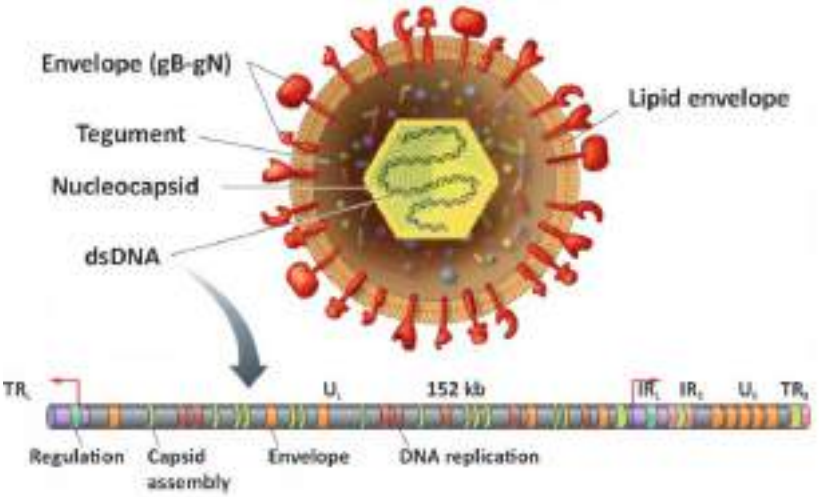

Figure 4. Schematic representation of HSV-1 (adapted from microbe notes). HSV-1 structure is composed by a dsDNA core surrounded by a nucleocapsid, a protein tegument and finally a membrane envelope rich of glycoproteins.

Following membrane fusion, viral tegument proteins are released in the cytosol and the viral nucleocapsid is directed to the nucleus along microtubules to release the viral genome. In the nucleus, viral DNA circularizes to transcribe immediate-early (IE), early (E) and late (L) viral gene products sequentially. The IE gene products regulate gene transcription and include ICP47 which is responsible for decreasing MHC-I expression in infected cells. The E gene products promote viral DNA synthesis catalyzing DNA replication or nucleic acid metabolism. Most of the L gene products are virion components such as capsid proteins, tegument proteins, and envelope glycoproteins [58]. Once viral DNA has replicated, progeny is assembled into nucleocapsids, acquires tegument proteins and is enveloped during budding with the inner nuclear membrane. The resulting capsids then bud again with the cytoplasmic membranes of the trans-Golgi network for secretion outside of the cell [59].
Approximately half of the genes are essential and encode for capsid proteins, viral DNA replication proteins, viral DNA cleavage/packaging proteins, and some envelope glycoproteins. HSV is unable to replicate with even a single dysfunction in an essential gene. The expression of non-essential genes enables the virus to replicate effectively in a variety of cell types under different conditions, resulting in the replication and survival of HSV in humans [54].

1.3.2.2.2 *HSV-1 engineering*

One effective technology for HSV-1 engineering exploits a bacterial artificial chromosome (BAC). The whole HSV-1 genome is cloned as a BAC plasmid which can subsequently be manipulated in E. coli [60]. BAC cloning requires the insertion of mini F plasmid sequences and antibiotic resistance genes into the viral genome.

An advantageous genetic engineering technology of HSV-1 is based on galK (galactokinase) recombineering which allows the introduction of the desired genetic modification into HSV-BAC DNA in bacteria. The advantages are twofold: first, the λ Red-mediated homologous recombination is carried out by recombinases transiently and inducibly expressed from the genome of an appropriate *E. coli* host strain, SW102. Second, galK is used as a positive and negative selection marker for the properly recombined HSV-BAC DNA recombinant since it is first inserted in the BC-HSV genome then, replaced by heterologous or viral sequences carrying the desired modification. This avoids the need to transform recombinase-expressing plasmids and enhances the efficiency of recovery of the final product by putting a negative selection on the constructs that still carry the galK marker [61]. Recombinant virus can be then rescued upon transfection in mammalian cells, susceptible and permissive to HSV. Many kinds of viral modifications can be obtained like point mutations, deletions/insertions, marker or transgene expression and changes to viral tropism [54].

The main goals of the engineering process are to prevent the infection of the nervous system, to enhance tumor-selectivity, to increase immunogenicity by adding genes expressing immunostimulatory mediators or counteract T-cell exhaustion [62].

1.3.2.2.3 *oHSV in HGG clinical trials*

Many oHSV have been engineered and evaluated in clinical trials showing efficacy and encouraging results (table 1).

Between the several HSV developed, the most investigated are:

- *G207*

G207 is the first oncolytic virus generated by genetic engineering technology. It was constructed from HSV-1 by deleting both copies of the γ34.5 gene with the aim of reducing viral growth and neurovirulence. The *E. coli* lacZ sequence was also inserted in the ICP6 gene encoding for ribonucleotide reductase to allow selective viral replication in dividing tumor cells [63].

While it was demonstrated that the virus could be safely administered without the development of encephalitis, other potential adverse events (AEs) were difficult to distinguish from disease-related symptoms. Because of a lack of convincing evidence of clinical efficacy, G207 clinical development has not yet reached the phase II stage of testing.

- HSV1716

HSV1716 was developed on the basis of the spontaneous variant 1714 of the Glasgow strain 17+. HSV1716 has a deletion of 759 bp in each copy of the RL1 gene which encodes for the γ34.5 protein.

This deletion prevent the replication of the virus within the CNS [64]. HSV1716 replicates only in actively dividing cells [65].
Clinical trial employing HSV1716 started more than 20 years ago but no progression from stage I early cytotoxicity safety has been made. This suggests that, despite its low cytotoxicity profile and its capability to proliferate in dividing cells, further improvements and eventually concomitant treatment are needed.

- *rQNestin34.5*

rQNestin34.5 is an oHSV based on F-strain HSV-1 and engineered by expressing ICP34.5 under a synthetic nestin promoter to drive robust tumor-selective viral replication [66].

- *M032*

M032 is a second generation oHSV that selectively replicates into tumor cells. It contains deletions for both alleles of the neurovirulence factor γ34.5 and is armed to express the stimulatory cytokine IL-12.

- *C134*

C134 is a recombinant oHSV where γ34.5 is deleted and which express the immunoreactive HCMV IRS1 gene [67].

- *G47Δ*

G47Δ was developed from G207 by deleting γ34.5 and α47 gene and inactivating insertion of LacZ into ICP6. Since α47 inhibits antigen presentation, its deletion is associated with an increased expression of MHC-I on virus-infected cells [68]. Todo and colleagues obtained important results with G47Δ which led to its approval as the first oncolytic virus product in Japan.

oHSV	***Clinical trial***
G207	Markert et al. 2000 [69]: phase I clinical trial on 21 patients affected by malignant glioma with recurrence despite surgery and radiation therapy. They received an initial dose at a single site of 10^6 PFU of G207 followed by a second dose up to 3 x 10^9 PFU at five sites. No toxicity or serious adverse events could unequivocally be ascribed to G207 and no patients developed encephalitis. Almost 73% of patients were already seropositive for HSV-1 and only patients injected with the higher dose seroconverted after G207 treatment. This study provided the safety of G207 with some indication for its use a potential therapy for malignant glioma.

	Markert et al 2009 [70]: phase Ib trial on 6 patients with recurrent malignant glioma. They were treated with an initial dose of 1.5 x 10^8 PFU followed by resection 2-5 days later and a second G207 injection of 10^9 PFU. Half of the patients that were negative for HSV-1 seroconverted after treatment. Despite no total or partial response occurred, antitumor activity was reported.
	Markert et al. 2014 [71]: phase I trial on 9 patients with recurrent malignant glioma. They received one dose in multiple sites of 10^9 PFU 24 hours before 5 Gy radiation. One third of them was seronegative for HSV-1 and only 1 seroconverted after treatment. Between seropositives, some had augmented antibody levels. Six out of 9 had stable disease or partial response for at least one time point.
HSV1716	Rampling et al. 2000 [72]: trial on high grade glioma patients (8 GBM and 1 anaplastic astrocytoma) who had relapsed following radical treatment who received up to 10^5 PFU. Eight out of 9 were HSV-1 seropositive and IgM and IgG titres didn't change significantly after HSV1716 administration. These patients had also a significant degree of immune incompetence. This trial showed that HSV1716 didn't induce adverse reaction nor reactivation or recrudescence of HSV. Four patients remained alive 24 months after the treatment.
	Papanastassiou et al. 2002 [73]: high grade glioma patients (11 recurrent and 1 newly diagnosed) with significative degree of impaired immunocompetence, received intratumoral injection of 10^5 PFU of HSV1716. This study had the aim to consolidate the non-toxicity of HSV1716 and to evaluate virus replication which was analyzed in tumor sample obtained after resection 4-9 days post treatment. They recovered HSV1716 from 2 patients and semi-quantitative PCR showed evidence of HSV DNA at distal tumor sites in 3 different patients. In this study, they also observed that the 2 negative patients for HSV seroconverted and 3 other patients showed and increased IgM and IgG response after treatment with HSV1716.
	Harrow et al. 2004 [74]: recurrent or newly diagnosed patients with high-grade glioma (6 recurrent and 6 newly diagnosed) were treated with 10^5 PFU of HSV1716 into 8-10 sites after brain surgery. Two out of 3 negative patients seroconverted after HSV treatment. There was no clinical evidence of toxicity. After treatment, 3/12 patients were clinically stable.
rQNestin34.5	Phase I unpublished trial to test the safety of rQNestin34.5 for the treatment of recurrent malignant glioma together with cyclophosphamide on 51 patients.
M032	Patel et al. [75]: design of a phase-I trial to investigate safety and tolerability of M032 in patients with recurrent or progressive high-grade glioma.

	Unpublished phase I-II clinical trial for the evaluation of M032 in combination with pembrolizumab is also ongoing on 28 patients with recurrent/progressive glioblastoma multiforme, anaplastic astrocytoma or gliosarcoma.
C134	Ongoing phase I unpublished trial on 24 patients with recurrent malignant glioma to test the safety and tolerability.
G47Δ	Todo et al 2022 [76]: Phase I-II trial to assess the safety and efficacy of G47Δ on 13 patients with recurrent or progressive glioblastoma. Patients were intratumorally treated with 2 doses of G47Δ between 5-14 days. A first cohort of 3 patients was treated with 2 doses of 3 x 10^8 PFU of virus. The second cohort and the phase II trial patients were treated with 2 doses of 10^9 PFU. Median OS was 7.3 months and the 1-year survival rate was 38.5% after last G47Δ administration. Three patients survived > 46 months, 1 complete response and 1 partial response were observed at 2 years.
	Todo et al 2022 [77]: phase II trial on 19 patients with residual or recurrent glioblastoma after radiation therapy and temozolomide. A total of 10^9 PFU per dose of G47Δ was administered intratumorally by MRI-guided stereotactic surgery at interval of 5-14 days for the 2 first administrations followed by up to 6 doses at interval of 4 +/- 2 weeks. After G47Δ administration, the 1-year survival rate was 84.2% and OS was 20.2 months. The best overall response in 2 year was the partial response of 1 patient and the stable disease for other 18 patiens.

Table 1. Description of clinical trials published or still ongoing on high grade gliomas treated with different oHSVs. Number of patients, treatment schedules, virus administration and main outcomes are summarized.

2 Previous studies of the research group

2.1 HGG murine model

Our laboratory developed two main mouse models of high-grade glioma, both based on the induction of PDGF-B overexpression. In particular, the model employed in my PhD studies was empowered to evaluate the efficacy of oncolytic HSVs. This model is based on the transduction of neural progenitor cells obtained from day 14 (E14) BALB/c mouse embryos transduced with a retroviral vector encoding for PDGF-B which is known to induce gliomas [78] and the red fluorescent protein dsRed. After 7 days of culture, these cells were injected into adult BALB/c brains and developed high grade gliomas (mHGG^{pdgf}). Tumor cell lines (mHGG^{pdgf} cells) were then obtained by tumor dissociation. These cells were also implemented for the expression of the human receptor HER2 (hHER2) [79]. The expression of hHER2 and oligodendroglial precursors markers such as, Nestin, Ng2 and Olig2 by tumor cells was

demonstrated by immunocytochemical analysis. Mice intracranially injected with mHGG^{pdgf}-hHER2 cells successfully developed mHGG^{pdgf} tumors which histologically resemble each other and human HGGs since they are characterized by quiet a compact structure and necrotic areas surrounded by highly proliferating cells forming pseudopalisades (Figure 5A) [79].

2.2 HSV-1 oncolytic virus R-LM113

2.2.1 R-LM113 in vitro

R-LM113 is a third generation, fully retargeted oHSV developed by our collaborators from University of Bologna. This oncolytic virus is detargeted from its natural receptors nectin-1 and HVEM and retargeted to hHER2 (Figure 5B). A single chain antibody fragment for hHER2 was located in the site of the viral envelopie glyocoprotein gD in order to lie in front of the nectin1-interacting surface. At the same time, the N-terminus was deleted from amino acid residues 6 to 38, described as important for nectin-1 and HVEM binding to achieve detargeting. This approach yielded an HSV recombinant simultaneously detargeted from HVEM and nectin1 and retargeted to hHER2. The infection by R-113 is detectable thanks to the expression of EGFP reporter gene, cloned in the viral genome.

R-LM113 demonstrated its selectivity for hHER2 expressing cells together with its inability to grow in nectin-1 and HVEM expressing cells. The hHER2-mediated infection was also confirmed by neutralization of infection experiments in which HER2 expressing cells were blocked with Herceptin (antibody against HER2) that prevented R-LM113 infection. Human HER2 also demonstrated its role in the cell-to-cell viral spread. The safety of R-LM113 was also evaluated in vivo by intracranial injection of nonobese diabetic/severe combined immunodeficient (NOD/SCID) mice, extremely sensitive to wild-type HSV [80]. The results demonstrated that the R-LM113 oncolytic virus is safe and it cannot infect and spread in normal brain tissue [81]. These results were also confirmed in the immunocompetent BALB/c mice, a strain susceptible to HSV infection [79].

2.2.2 R-LM113 in mHGG^{pdgf} mouse model

The efficacy of R-LM113 was demonstrated on the aforementioned mouse model of high grade glioma induced by the expression of PDGF-B and whose cells express hHER2. A first experiment was performed on NOD/SCID mice coinjected with mHGG^{pdgf}-hHER2 cells and mHGG^{pdgf}-hHER2 cells previously infected in vitro with R-LM113. Mice treated with R-LM113 showed an improved survival time with a median survival time of 119 days vs 55 days of the control group. Of the 12 mice treated, 2 survived until the end of the planned experiment (160 days). Analyses of their brain demonstrated that one bore a dsRed positive tumor with the absence of EGFP signal while the other mouse showed a very small region of dsRed- and EGFP-positive cells only after dissection, suggesting that the ongoing infection was successfully counteracting the tumor growth.

In another experimental set, mice were treated 45 days post tumor transplantation. Treated mice receive 3 x 10^5 PFU of R-LM113 intracranially while controls received an equal amount of UV-inactivated virus. Even in this case, treated mice showed an increased survival if compared to the control group [81].
Given the encouraging results, the efficacy of R-LM113 was then tested on an immunocompetent model of mHGG.
A first experiment was performed by coinjecting mHGG^{pdgf}-hHER2 cell with mHGG^{pdgf}-hHER2 cells previously infected with R-LM113 in BALB/c mice. Treated mice showed an increased survival of 77 days compared to 46 days of the control group. Two mice survived until the end of the experiment and, when sacrificed, the analysis of their brains showed that one mouse had a dsRed- EGFP-positive tumor, suggesting that the virus was still acting on the tumor cells and the other mouse appeared tumor free.
Another experiment was performed by treating mHGG^{pdgf}-hHER2 bearing mice with R-LM113 26 days post tumor injection. Despite all the mice died because of ds-Red positive tumors, their median survival was still significantly increased and 6 out of 16 mice had an oHSV infection going on [79].

2.3 HSV-1 oncolytic virus R-115

2.3.1 R-115 in vitro

To improve the therapeutic efficacy of R-LM113 an improved oHSV was developed using R-LM113 as a backbone (Figure 5B). The cassette coding for murine interleukin 12 (mIL12) was engineered under the control of pCMV in the US1-US2 intergenic region, generating R-115.
The murine IL12 was chosen because it is known that it can strongly stimulate the immune system. Murine IL12 loses its power when administered systemically because of its toxicity, while locoregional delivery via viral vector proved to be a useful alternative [82].
My colleagues showed that R-115 maintained the tropism previously exhibited by R-LM113. Similarly, it also replicated selectively in hHER2 expressing cells. The amount of mIL12 were also tested. The supernatant of R-115 infected cells was collected 24 hours after infection and analyzed by ELISA, revealing a concentration of mIL12 between 100 and 400pg/10^5 cells.

2.3.2 R-115 in mHGG^{pdgf} mouse model

The in vivo efficacy of R-115 was demonstrated by our research group and its activity was compared to the parental virus R-LM113. Mice inoculated with mHGG^{pdgf}-hHER2 cells were treated by intracranial injection of 10^8 PFU of R-115 (high dose) or 2 x 10^6 of R-115 or R-LM113 (low dose) 21 days post tumor implantation while the control arm received irradiated virus. The oHSV treatment confirmed to increase the median overall survival when compared to controls. Despite there was no difference between high dose and low dose of R-115, and between R-LM113 and R-115 treated mice,

a dramatic difference was appreciable in terms of long survivors. While in the R-LM113 arm all mice were inevitably sacrificed, about 27% of R-115 treated mice survived 100 days after virus injection (Figure 5C). Of these long survivors, 2 were sacrificed and showed no sign of tumor and 2 were reinoculated with mHGG^{pdgf}-hHER2 and survived for other 220 days. They were then additionally transplanted with mHGG^{pdgf} cells. Still, they didn't develop any tumor, suggesting the acquisition of anti-tumor immune resistance [83].

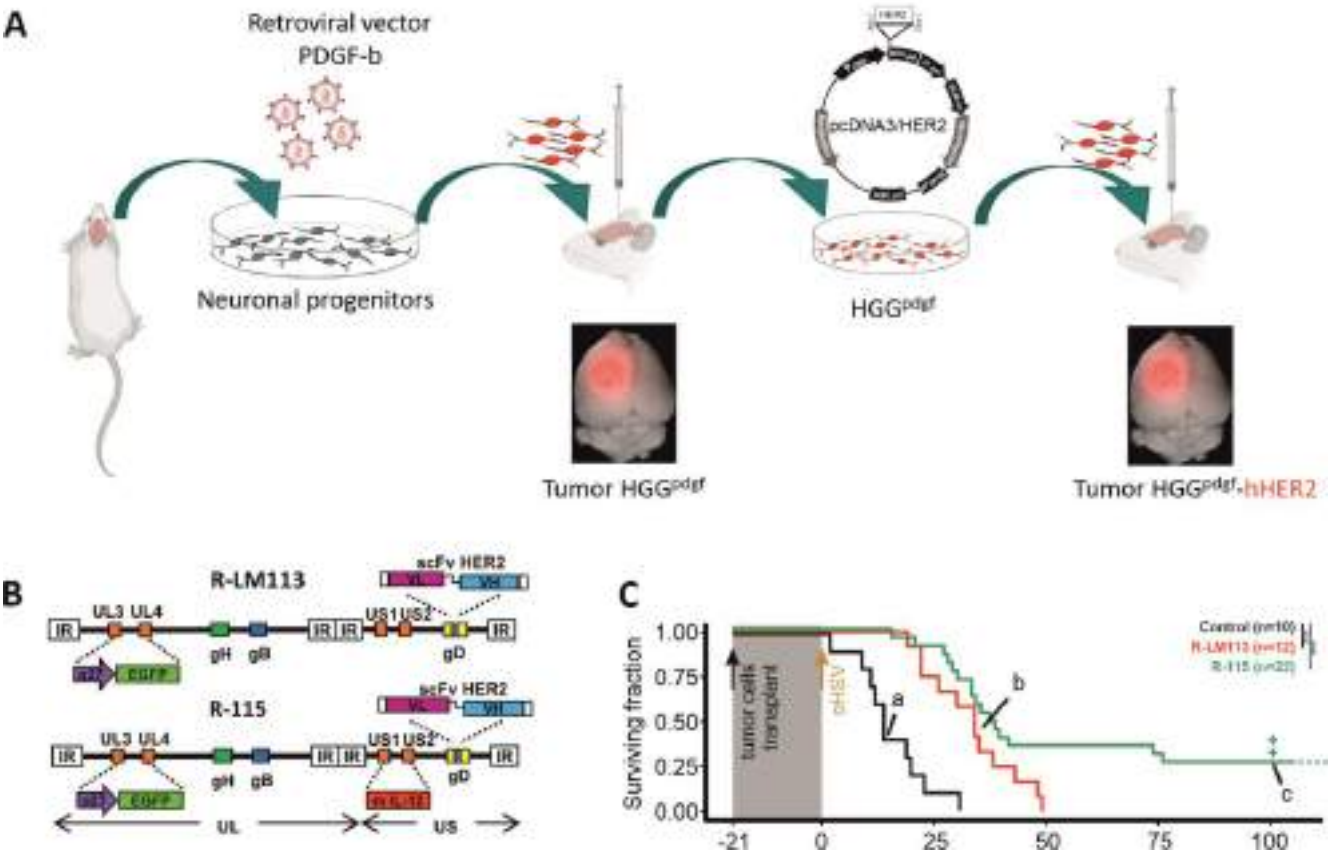

Figure 5. Schematic representation of mHGG^{pdgf} model: neural progenitors from E14 are infected with retroviral vector coding for PDGF-B and dsRed and then orthotopically inoculated into BALB/c mice. Murine HGGs generated were dissociated and transfected with a plasmid coding for human HER2 and then reinoculated into BALB/c mice, developing mHGG^{pdgf}-hHER2 tumors, A. Schematic backbone of R-LM113 and R-115. Both viruses carry the insertion of BAC sequences and EGFP gene in the UL3-UL4 intergenic regions, the deletion of aa 6-38 in gD and its replacement with scFv targeting hHER2. R-115 also carries the mIL-12 gene (Leoni V. et al. 2018), B. Kaplan-Meier curve of R-115 treated mice (green) compared to R-LM113 (red) and control mice (black), C.

3 Rationale

New possible therapies for the treatment of high-grade glioma are constantly developed and under investigation but malignant gliomas' heterogeneity still makes them resistant to several approaches and many therapies are limited to only few patients.

My PhD studies were focused on proving R-115, an oncolytic HSV targeting hHER2 and expressing murine IL12, as a convincing therapy for the treatment of high-grade glioma.

To evaluate the translatability of R-115 to the clinic, my main goal was to investigate the efficacy of R-115 and to characterize its induced immune response in a patient-like scenario.

A second aim was to evaluate the efficacy of ex vivo stimulated immune cells as an alternative possible therapy.

4 Results 1: R-115 as a potential therapy for glioblastoma

4.1 R-115 efficacy is similar in mHGG^{pdgf}-hHER2- and mHGG^{pdgf}-MIX tumor-bearing mice

Our group previously demonstrated the efficacy of R-115 (an oncolytic virus targeting the human receptor HER2 and coding for the murine IL12) for the treatment of mHGG^{pdgf}-hHER2 tumors [83]. Despite the robust results obtained, it is well known that glioblastoma are commonly heterogeneous tumors where not necessarily all the cells express hHER2. To evaluate the translatability of R-115 treatments against HGG, we tested the virus in a new model based on a mixed population of mHGG^{pdgf}-hHER2 which better represents the variable hHER2 expression found in patients. This new model was compared to the previously tested of mHGG^{pdgf}-hHER2. BALB/c mice were orthotopically transplanted with 2 x 10^4 mHGG^{pdgf}-hHER2 cells (n = 44) or with 2 x 10^4 mHGG^{pdgf}-hHER2/mHGG^{pdgf} cells, herein after called mHGG^{pdgf}-MIX; n = 47). Mice were then randomized and treated with R-115 (10^6-10^7 PFU). Control group (n = 48) received an equivalent volume of γ-irradiated virus. At the first signs of suffering or neurological symptoms, mice were sacrificed. As shown in Figure 6A-B, median overall survival of mHGG^{pdgf}-hHER2 bearing mice (58.5 days) confirmed to be increased compared to the control group (33.5 days, p-value < 0.001), as expected from previous published data [84]. Remarkably, the overall survival of mHGG^{pdgf}-MIX bearing mice was at least as good as the mHGG^{pdgf}-hHER2 arm (67 days, p-value < 0.001).

While all mice from control group invariably developed symptoms that required their euthanasia, about one third of mice from both mHGG^{pdgf}-hHER2 and mHGG^{pdgf}-MIX groups was still alive after 120 days and the final fraction of rescued mice was of 27% and 22%, respectively.

These remarkable results confirm the ability of oncolytic immunovirotherapy to induce an immune response in addition to the direct lytic effect of R-115 on hHER2 targetable cells, necessarily promoting the killing of mHGG^{pdgf} cells through other players.

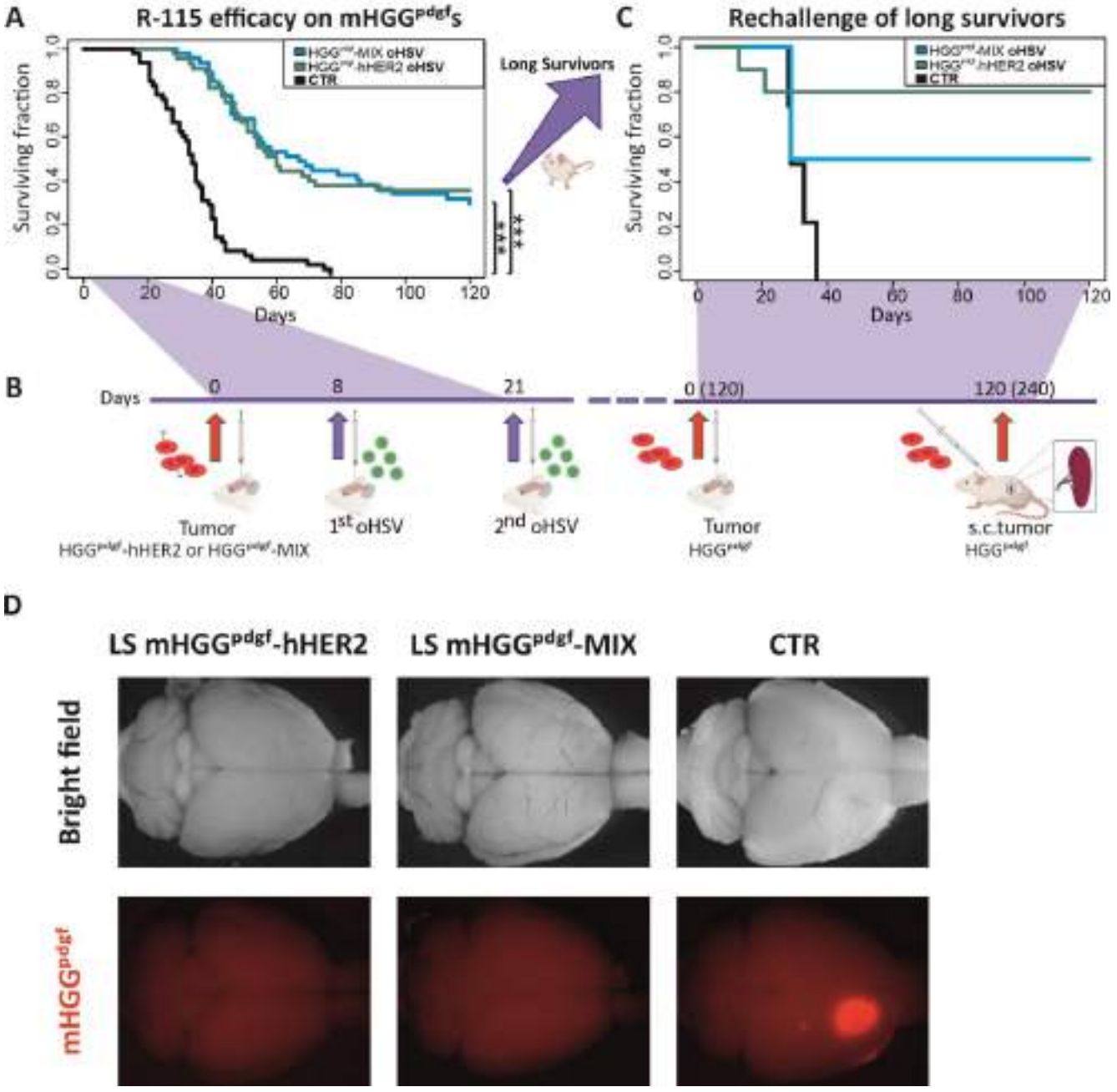

Figure 6. Kaplan-Meyer survival curves of mice transplanted with mHGG^{pdgf}-hHER2 (green, n = 44) and with mHGG^{pdgf}-MIX (blue, n = 47) and treated with R-115. The black line represents the control mice transplanted that received an injection with γ-irradiated R-115 (n = 48). *** Rank test, p-value<0.001, A. Schematic representation of the treatment's timeline: mice received an orthotopic transplantation of mHGG^{pdgf}-hHER2 cells or mHGG^{pdgf}-MIX cells. After 8 and/or 21 days, they received an intracranial injection of R-115. Mice survived 120 days post tumor injection received a second transplant of mHGG^{pdgf} cells. After other 120 days, survived mice received a subcutaneous injection of mHGG^{pdgf} cells and were then sacrificed 7 days after. B. Kaplan-Meyer survival curve of mice rechallenged with secondary transplantation of mHGG^{pdgf} cells after 120 days from primary tumor transplantation, C. Example of dorsal images of brains of long surviving mice originally transplanted with mHGG^{pdgf}-hHER2 cells or mHGG^{pdgf}-MIX cells treated with R-115 or inactivated virus and then retransplanted with mHGG^{pdgf} cells. In LS mice, the absence of red (dsRed from tumor cells) and green (EGFP from oHSV) signal suggests the eradication of the tumor mass and the clearance of R-115 while the control mouse has a clear dsRed positive tumor mass.

4.2 Evaluation of R-115 multiple treatment schedules

R-115 treatment of mHGG^{pdgf}-hHER2

Previously published data from our laboratory demonstrated that treatment with R-115, when administered 21 days post tumor transplantation, prolonged survival and eradicated glioblastoma in about 27% of mHGG^{pdgf}-hHER2 bearing mice [83]. Here we wanted to investigate if modulating the schedule treatment could have an impact on overall survival and tumor eradication. To do so, we treated mice after 8 days (single-early treatment; herein after labeled as E), 21 days (single-late treatment; labelled as L) or 8 and 21 days post tumor injection (early + late treatment; labelled as EL). BALB/c mice were orthotopically injected with 2 x 10^4 mHGG^{pdgf}-hHER2 cells. Mice were then randomized and treated with R-115 (10^6-10^7 PFU). Control groups received an equivalent volume of γ-irradiated virus.

As shown in Figure 7A, median overall survival times of all mHGG^{pdgf}-hHER2 bearing mice was 49 days in E group (n=16), 55 days in L group (n = 14) and 70 days in EL group (n = 14). Overall survival of all tree arms was increased in all log-rank test comparisons of each treated group versus the control group (p-values < 0.001). No significant difference was found between all the treated groups.

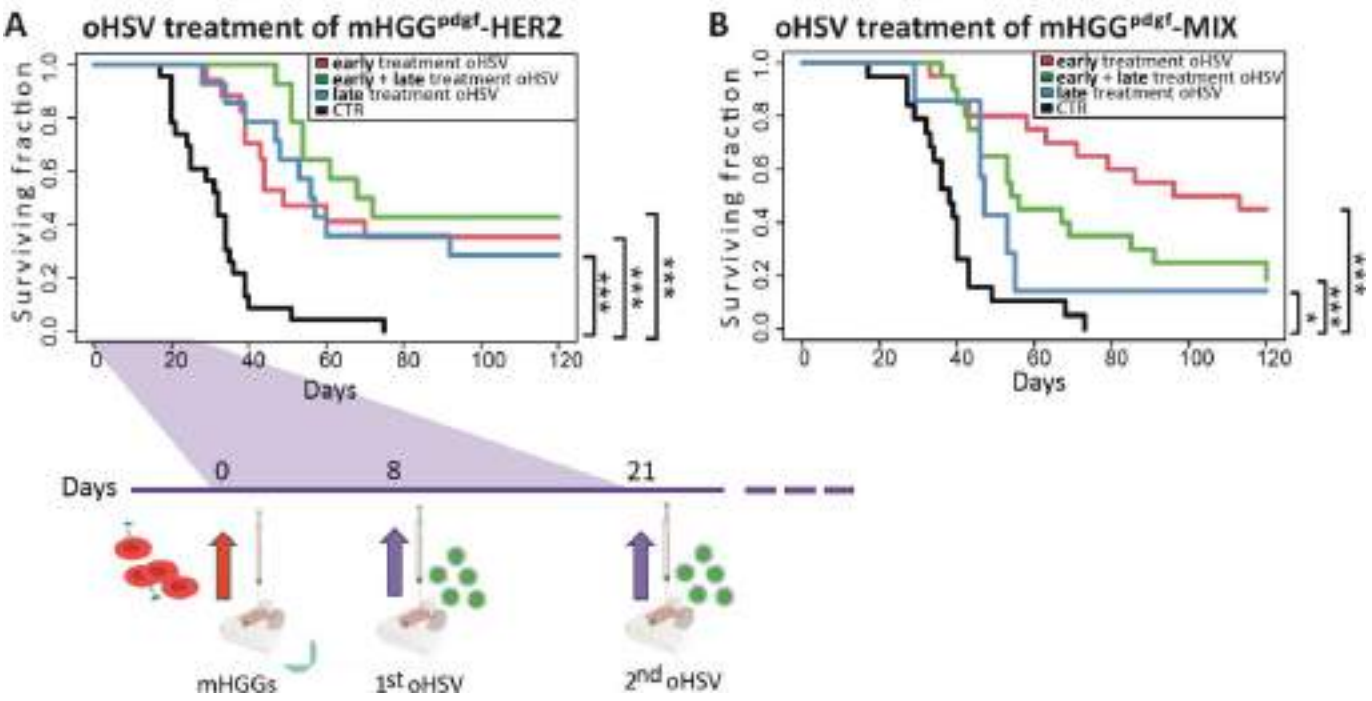

Figure 7. Kaplan-Meyer survival curves of mice transplanted with mHGG^{pdgf}-hHER2 and treated with different R-115 schedules: early treatment at 8 days (red, n = 16), early + late treatment at 8 and 21 days (green, n = 14) and late treatment at 21 days (blue, n = 14). The black line represents the control mice that receive an injection with γ-irradiated R-115 (n = 22), A. Kaplan-Meyer survival curves of mice transplanted with mHGG^{pdgf}-MIX and treated with different R-115 schedules: early treatment at 8 days (red, n = 21), early + late treatment at 8 and 21 days (green, n = 20) and late treatment at 21 days (blue, n = 7). The black line represents the control mice that receive an injection with γ-irradiated R-115 (n = 23), B. * Rank test, p.value < 0.05. *** Rank test, p-value<0.001

R-115 treatment of mHGG^{pdgf}-MIX

The same schedules were tested on mHGG^{pdgf}-MIX bearing mice. We orthotopically injected BALB/c mice with 2 x 10^4 mHGG^{pdgf}-MIX. After randomization, mice were treated with R-115 at 8 days (n = 20), 21 days (n = 7) or 8 and 21 days (n = 20) post tumor injection. The result obtained were overlapping those obtained with the mHGG^{pdgf}-hHER2. Overall survival of all tree arms was increased compared to control group. Log-rank- test p-value in both the comparison of E and EL versus the control group was smaller than 0.001. The p-value in the comparison between L and the control group appeared higher (p=0.05) although no significant differences emerged when the overall survival in the three arms were directly compared one to the other. Despite no statistically significant difference, the E group tended to have a better outcome and median overall survival (Figure 7B).

Rechallenge

To evaluate the immune memory against tumor cells induced after R-115 treatment, we performed a rechallenge experiment by intracranially infusing glioblastoma cells into the contralateral (right) hemisphere of mice that survived more than 120 days after tumor transplant. For the rechallenge, we infused 2 x 10^4 mHGG^{pdgf} cells (without hHER2 transgene) both in the surviving mice which received in their first transplant mHGG^{pdgf}-hHER2 (n = 4) and in those which received the mHGG^{pdgf}-MIX (n = 2). No additional R-115 was administered and a control group was also injected (n = 4). After 120 days 3 out of 4 of originally transplanted mHGG^{pdgf}-hHER2 mice and 1 out of 2 of mHGG^{pdgf}-MIX were still alive. Surviving mice, herein referred to as long survivors, were sacrificed and their brains were checked for the presence of tumor (Figure 6B-D). No dsRed positive cells were found in treated mice, suggesting that R-115 treatment was not only capable to eradicate the first transplanted tumor but it also induced an immune memory which prevented the development of a glioma after the second transplant.

Considering the lack of differences between different schedule arms both for the mHGG^{pdgf}-hHER2 and for the mHGG^{pdgf}-MIX treated tumors and between mHGG^{pdgf}-hHER2 and mHGG^{pdgf}-MIX tumors, from now on, we refer at mice simply as treated groups vs controls.

4.3 Characterization of the immune component of long-survivors

To analyze the reactivity against glioblastoma cells of the immune system of long survivors (LS), one week before the sacrifice, we boosted them by a subcutaneous injection of 5 x 10^5 mHGG^{pdgf} cells n = 4). In parallel, as a control, 4 age-matched naive mice received the same subcutaneous injection (scNAIVE). Together with these two groups, we also analyzed the basal reactivity of 2 aged-matched NAIVE mice (NAIVE).

After 7 days from subcutaneous injection, we sacrificed all the mice and collected their splenocytes and brains. Splenocytes were partly analyzed immediately (t0) and partly co-cultured with mHGG^{pdgf}-hHER2, mHGG^{pdgf} or with syngeneic fibroblasts as control for 3 (t3) and 7 days (t7).

4.3.1 Splenocytes proliferation

To evaluate any difference in proliferation between splenocytes derived from LS and control groups (scNAIVE and NAIVE) when co-cultured with mHGG^{pdgf}-hHER2, mHGG^{pdgf} or autologous fibroblast (applied as internal normalizer), splenocytes were stained with CFDA-SE at t0. After 7 days, cells were stained with CD45 together with CD4, CD8 or CD19 to characterize the proliferation of T helper lymphocytes, cytotoxic T lymphocytes (CTL) and B cells, respectively.

All the tree components of CD4, CD8 and CD19 originated from LS proliferated more than the splenocytes from NAIVE and scNAIVE mice (LS vs scNAIVE: CD4 p-values < 0.05, CD8 p-value < 0.05, CD19 p-value < 0.05) when co-cultured with mHGG^{pdgf}-hHER2 cells (Figure 8A).

We obtained similar results when we co-cultured splenocytes with mHGG^{pdgf} cells. CD4, CD8 and CD19 from LS proliferated more than scNAIVE (LS vs scNAIVE: CD4 p-values < 0.05, CD8 p-value < 0.05, CD19 p-value = 0.07) and then the NAIVE group (Figure 8B).

On the other hand, there was no difference between the extent of proliferation of splenocytes co-cultured with mHGG^{pdgf}-hHER2 or mHGG^{pdgf} tumor cells.

4.3.2 ELISpot analysis of IFNγ released by splenocytes

IFNγ is a pleiotropic cytokine that coordinates several biological responses, primarily involved in host defense and immune surveillance but also the establishment of adaptive immunity [85].

IFNγ acts trough different mechanism of action including the inhibition of actively dividing cells, induction of apoptosis, increase of the immunogenicity by inducing upregulation of MHC-I and MHC-II and inhibition of angiogenesis [86].

Since IFNγ is a marker of immune stimulation, we evaluated its release by splenocytes to determine their level of activation after tumor subcutaneous rechallenge. At t0, we harvested cells from LS, scNAIVE and NAIVE spleens and immediately plated them on IFNγ pre-coated ELISpot plates.

After 48 hours of incubation, we removed cells, washed the plates and stained with a secondary IFNγ antibody. After revelation, number of spots was evaluated (Figure 8C). ELISpot analysis revealed that one week after subcutaneous injection, splenocytes from LS were strongly reactivated releasing a large amount of IFNγ while scNAIVE and NAIVE groups displayed a minimal number of spots indicating almost no IFNγ release (LS vs scNAIVE p-value < 0.05).

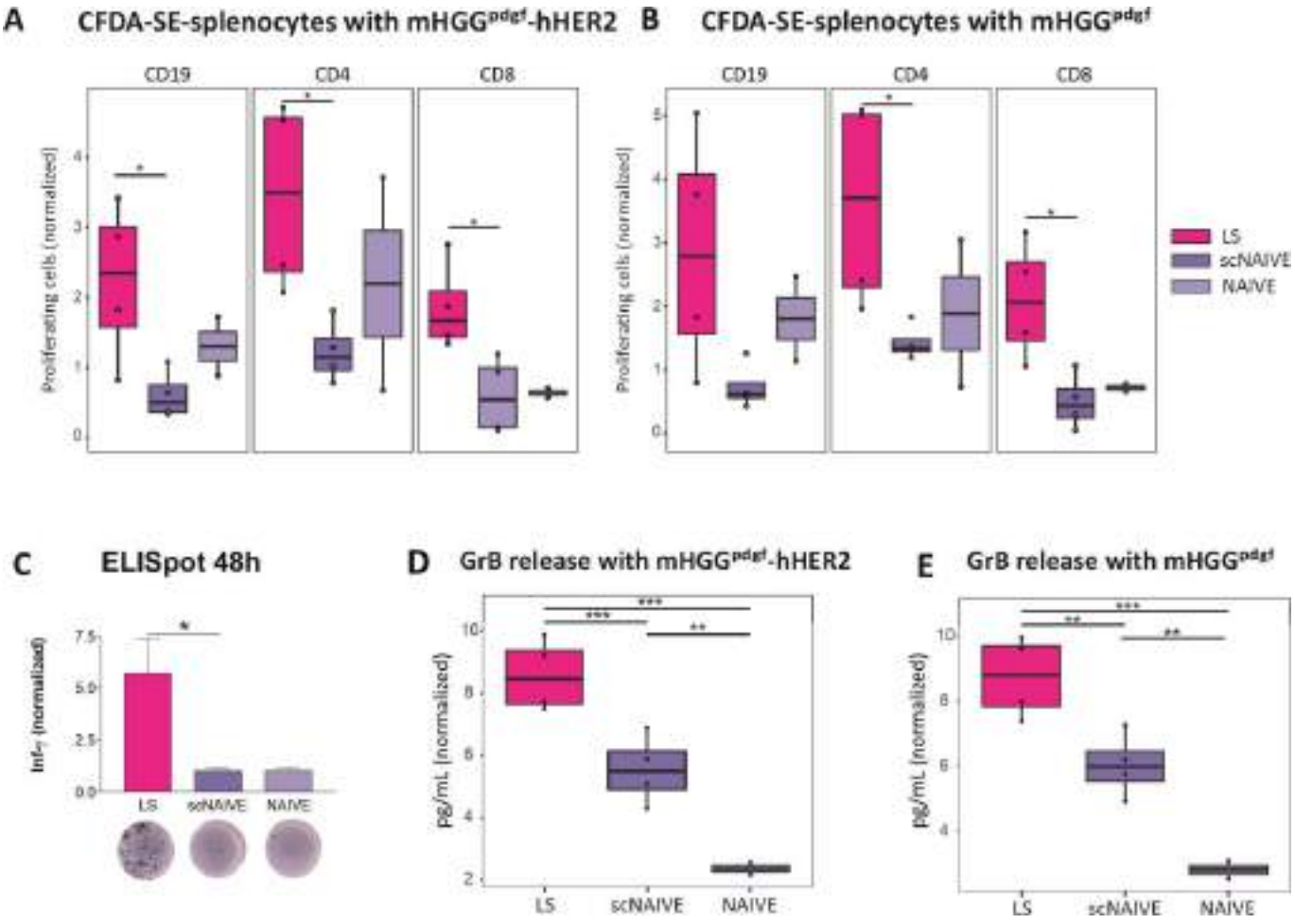

Figure 8. Proliferation of CFDA-SE stained splenocytes co-cultured with mHGG^{pdgf}-hHER2 (A) or mHGG^{pdgf}-MIX (B), normalized on splenocytes co-cultured with autologous fibroblast. IFNγ release by splenocytes after 48h, C. Granzyme B released by splenocytes co-cultured with mHGG^{pdgf}-hHER2 (D) or mHGG^{pdgf}-MIX (E). *** p-value<0.001, ** p-value<0.01, * p-value<0.05 LS (violet), scNAIVE (lilac) or NAIVE (light lilac)

4.3.3 Release of Granzyme B as cytotoxicity marker

Stimulation of NAIVE CD8 CTLs and NK cells with cytokines and/or specific antigens cause their differentiation into killer cells which require the rapid synthesis, safe trafficking and storage of a large amount of perforins and granzymes. Granzyme B is the most powerful pro-apoptotic granzyme as its ability to cleave target cell proteins mimics caspase and induced rapid and effective cell death [87].

To evaluate the activation of CTLs and NK we analyzed the amount of Granzyme B released in the supernatant of splenocytes derived from LS, scNAIVE and NAIVE co-cultured with mHGG^{pdgf}-hHER2, mHGG^{pdgf} or autologous fibroblasts (applied as internal normalizer). Supernatants collected at t7 were plated on ELISA plates pre-coated with Granzyme B antibody. After an overnight incubation, plates were washed and stained with a secondary antibody against Granzyme B and the amount of released

Granzyme B was evaluated. Supernatant derived from co-culture of mHGG^{pdgf}-hHER2 or mHGG^{pdgf} cells with LS mice contained a significantly higher amount of secreted Granzyme B compared to scNAIVE and NAIVE (Figure 8D-E).
Despite there were no detectable differences between scNAIVE and NAIVE group in proliferation and IFNγ analyses, a variation of granzyme B release was visible (mHGG^{pdgf}-hHER2 co-cultures: scNAIVE vs NAIVE p-value < 0.01; mHGG^{pdgf} co-cultures: scNAIVE vs NAIVE p-value < 0.01). This small amount of granzyme B released by splenocytes from scNAIVE could be explained by an innate response of the immune system, probably associated to NK cells, which is more appreciable in a subcutaneous injection.

4.4 Characterization of the effects induced by the immune system on tumor cells

4.4.1 LS splenocytes mediated tumor cells death

Reduction of PDGFR-α expressing tumor cells

To elucidate if the active status of splenocytes corresponded to an active killing effect on tumor cells, we investigated the consequences of co-cultures on the survival of the tumor component. To evaluate tumor cell death, we get advantage of PDGFR-α ubiquitous expression by tumor cells. We determine the fraction of living cells in the co-culture versus the tumor cells alone. All the cytofluorimetric measures were performed using a PDGFR-α-negative NIH/3T3 spike-in as normalizer. At t7, co-culture where stained with anti-PDGFR-α and anti-CD45 antibodies to discern tumor cells, NIH/3T3 and splenocytes. As shown in Figure 9A, the amount of tumor cells was strongly reduced in tumor cells co-cultured with activated splenocytes from LS but not from scNAIVE or NAIVE, confirming that the release of Granzyme B was effectively associated to tumor cell reduction.

Reduction of luciferase expressing tumor cells

To consolidate the specific targeting of new antigens besides HER2, we double checked the cytotoxic activity of splenocytes on mHGG^{pdgf} cells engineered to induce the expression of luciferase reporter gene (mHGG^{pdgf}-LUC). We evaluated the luciferase-mediated signal in tumor cells at t7 after co-culture of splenocytes with mHGG^{pdgf}-LUC cells. Again, as shown in Figure 9B, when co-cultured with LS, the amount of luciferase producing tumor cells is reduced if compared to tumor cells co-cultured with scNAIVE or NAIVE splenocytes.

4.4.2 LS splenocytes restore MHC-I expression on tumor cells

Glioblastoma is well known as an immunosuppressive cold tumor, in part due to MHC-I downregulation, reflected also in our model where both mHGG^{pdgf}-hHER2 and mHGG^{pdgf} cells express extremely low levels of MHC-I [86]. To investigate if LS-derived stimulated splenocytes secreting IFNγ could restore MHC-I on tumor cells, we stained co-cultured tumor cells to evaluate the MHC-I expression at t3. The analyses showed that MHC-I was completely restored on both mHGG^{pdgf}-hHER2 and mHGG^{pdgf} cells when co-cultured with LS splenocytes while the presence of scNAIVE or NAIVE splenocytes had low or no effect on the complex expression (Figure 10C-D).

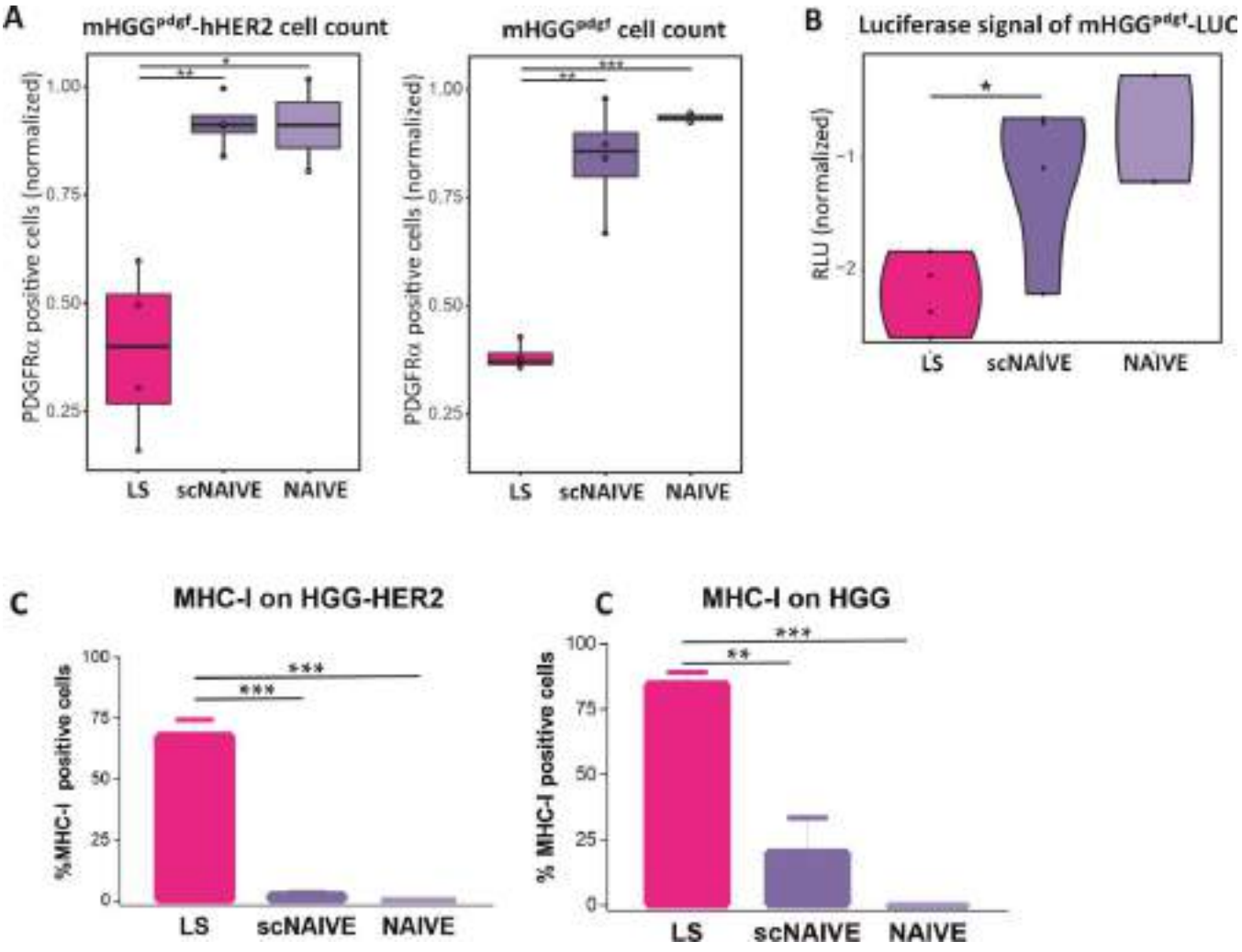

Figure 9. Percentage of PDGFRα+ cell left after co-culture of splenocytes with mHGG^{pdgf}-hHER2 or mHGG^{pdgf} cells, A. Luciferase signal released by splenocytes after co-culture with mHGG^{pdgf}-LUC cells, normalized on mHGG^{pdgf}-LUC cell alone, B. MHC-I expression at t3 on mHGG^{pdgf}-hHER2 tumor cells (C) or mHGG^{pdgf} (D) after co-culture with splenocytes, normalized on tumor cells alone. LS (violet), scNAIVE (lilac) or NAIVE (light lilac).

5 Results 2: Splenocytes ex vivo stimulation and training against mHGG^{pdgf} cells

According to the results obtained with the in vivo treatment of mHGGs with R-115, we wanted to investigate if a similar immune activation could be reproduced ex vivo and employed in vivo as a therapy.

5.1 Setting up of activating culturing conditions

To reproduce an in vivo antitumor environment, the first step was to generate activated lymphocytes.
We initially obtained fresh splenocytes from the spleen of BALB/c NAIVE mice. To induce T cells activation, Dynabeads Mouse T-Activator CD3/CD28 and the immune modulatory cytokines IL-2 and IL-15 were added to the medium.
Several combinations of Dynabeads and interleukins were investigated before getting to a final "Mix Beads" comprising 30U/mL IL-2, 10ng/mL IL-15 and a bead to cell ratio of 1:1.
To evaluate the proliferation induced by the Mix Beads, we stained splenocytes immediately after their collection from the spleen with CFDA-SE. Splenocytes without Mix Beads were used as negative control.
As shown in Figure 10A, after three days of culture (t3), the majority of splenocytes without Mix Beads died while the splenocytes with the Mix Beads not only survived but also replicated, as shown by cells shape and the CFDA-SE staining (Figure 10B).

5.2 Activated splenocytes enhance tumor cells death of oHSV-infected tumor cells

To evaluate if activated splenocytes could kill tumor cells, splenocytes were co-cultured for 2 weeks with tumor cells infected with R-115. R-115 encoded EGFP marker was used to assess the amount of living tumor. In this setup, the surviving fraction of R-115-infected mHGG^{pdgf}-hHER2 cells alone or co-cultured with activated splenocytes was monitored during time. Compared to R-115-infected mHGG^{pdgf}-hHER2 cells alone, the EGFP signal from co-cultured tumor cells decreases over time (Figure 10C), suggesting a synergistic role of activated splenocytes in the killing of tumor cells.

5.3 MHC-I recovery on tumor cells

Fresh splenocytes were cultured alone, with mHGG^{pdgf}-hHER2 or mHGG^{pdgf}-hHER2-oHSV cells for 2 weeks in a Mix Beads medium condition. Splenocytes were then sorted and co-cultured for 3 additional days with mHGG^{pdgf}-hHER2 or mHGG^{pdgf} cells to estimate their capability to restore MHC-I expression after their 2 weeks period of stimulation.
As shown in Figure 10D, flow cytometry analysis reveals that, despite MHC-I is almost not expressed on tumor cells, the 2 weeks stimulating environment is enough to restore MHC-I expression in tumor cells co-cultured in all conditions.

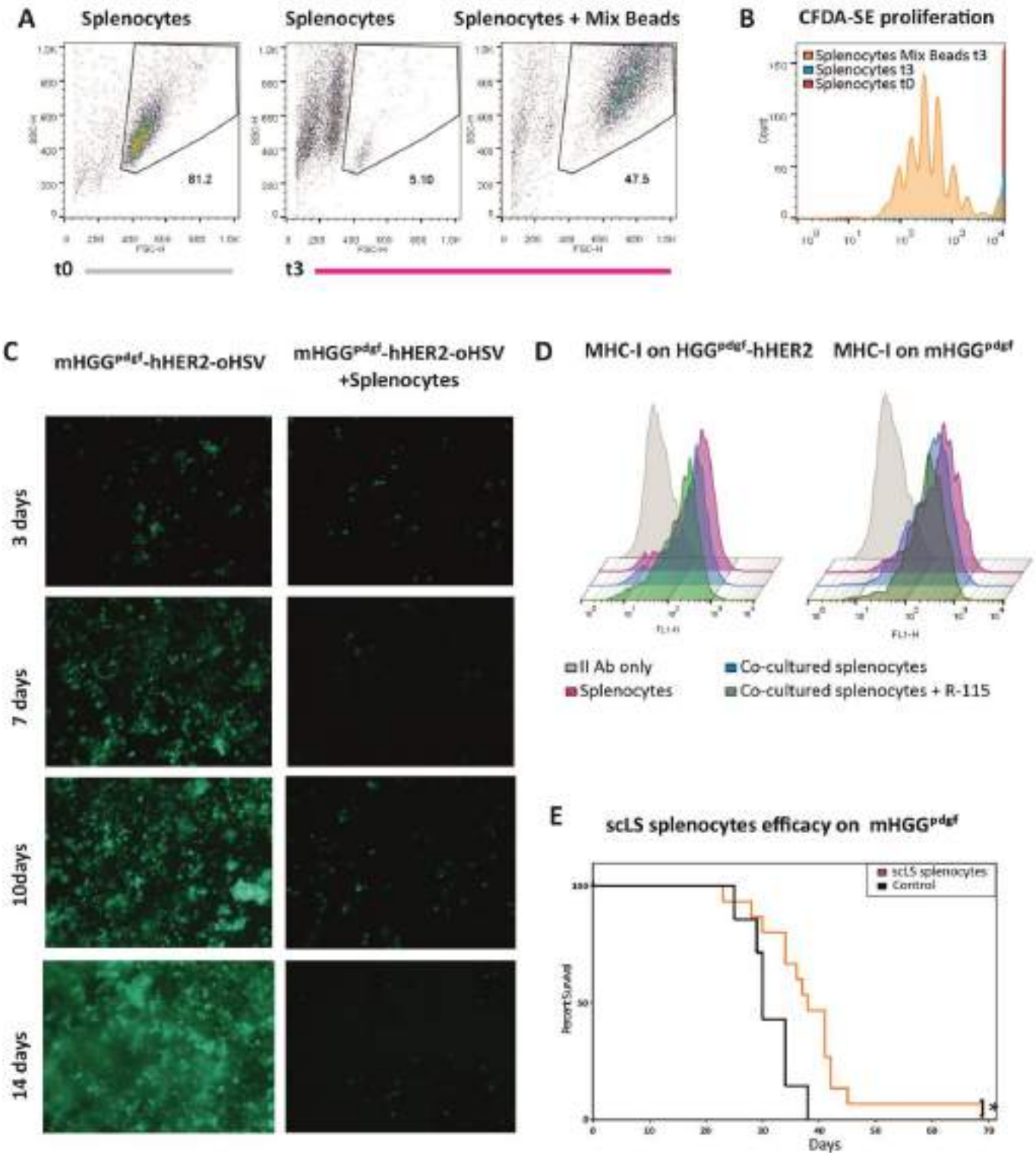

Figure 10. Flow cytometry analysis of physical parameters of NAIVE splenocytes at t0, A. CFDA-SE staining of NAIVE splenocytes at t0 and t3 alone or with Mix Beads medium, B. EGFP signal of mHGG^{pdgf}-hHER2 cells alone or co-culture with splenocytes activated with Mix Beads, C. MHC-I signal on mHGG^{pdgf}-hHER2 or mHGG^{pdgf} at t3, D. Kaplan-Meier of mHGG^{pdgf} bearing mice treated 8 days post tumor injection with activated splenocytes originated from LS mice, E. *p-value<0.05

5.4 Splenocytes from LS increase survival of mHGG^{pdgf} bearing mice

A preliminary experiment was conducted in vivo to evaluate the therapeutic potential of activated splenocytes. In particular, freshly collected splenocytes derived from 4 LS were co-cultured with Mix Bead cocktail for two weeks. Murine HGG^{pdgf} bearing mice were then treated with intracranial injection of 1.5 x 10^6 splenocytes 8 days post tumor transplantation.

Mice were monitored and sacrificed at the first signs of suffering or neurological symptoms. Figure 10E shows that a single treatment with activated splenocytes increased the overall survival of mHGG^{pdgf} bearing mice (38 days) if compared to the control group (30 days), (p-value < 0.05).

6 Methods

6.1 R-LM113

R-LM113 is an engineered HSV-1 kindly provided by the group of Prof. Campadelli Fiume from the university of Bologna. Briefly, the detargeting of gD was performed by replacing it with the insertion of the single chain HER2 ligand in other to target and infect specifically HER2 expressing cells. The cassette encoding for EGFP was also inserted into the BAC.

6.2 R-115

As for the other investigated virus, R-115 was developed by the group of the Prof. Campadelli Fiume. R-115 was improved from R-LM113 with the insertion of the cassette coding for murine interleukin 12 (mIL12) which was engineered under the control of pCMV in the US1-US2 intergenic locus. The final engineered genome included BAC sequence, the reporter EGFP gene, deletion of aa 6-38, scHER2L insertion, and mIL12 cassette.

6.3 Animal procedures - Murine model of mHGG^{pdgf}

All animal procedures were approved by internal committee for protection of animals used for scientific purposes (OPBA) of IRCCS Ospedale Policlinico San Martino and by the Italian Ministry of Health according to the Italian law D. lgs. 26/2014 and the European Directive 2010/63/EU of the European Parliament. The experiments were performed with the BALB/c mouse strain using animals of either sex. Mice were randomly assigned to the different experimental arms by assigning them a unique ID. The animals that did not survive surgery procedures were excluded from the experiment.

Tumors were implanted by injecting a suspension of a total of 2×10^4 mHGG^{pdgf} and/or mHGG^{pdgf}-hHER2 cells in adult mouse brains using a Hamilton syringe (Bregma coordinates: anterior–posterior, 1.0 mm anterior; lateral, and 2.5 mm below the skull surface). After 8 and/or 21 days post tumor implantation, mice were treated with 1-3 μL of oHSV preparation, containing 10^6-10^7 PFU of R-115. After 120 days post tumor transplantation, a rechallenge was performed by injecting a suspension of 2×10^4 mHGG^{pdgf} cells in the contralateral hemisphere. Animals were monitored daily and were sacrificed at first signs of suffering or neurological symptoms. Animals that didn't show any symptoms 120 days after the rechallenge were considered long-survivors (LS).

Subcutaneous injection of 5×10^5 mHGG^{pdgf} cells was administered to LS mice and a control group of NAIVE age-matched mice. All these mice, together with 2 age-matched NAIVE were sacrificed after 7 days.

When treated with activated splenocytes, mHGG^{pdgf} bearing mice were intracranially injected with 1.5×10^6 splenocytes 8 days post tumor transplantation.

Brains were photographed by fluorescence stereomicroscope (Wetzlar). Murine HGG^{pdgf} cells and R-115 were engineered to express the fluorescent reporters DsRed and EGFP respectively. Therefore, a

red and/or green fluorescent signal was photographed as indicative of the presence of tumor cells and oHSV.

Survival curves were determined using Kaplan–Meier survival between groups and compared by the log-rank test. The minimum sample size was preliminary established based on log-rank power analysis, assuming an effect size HR ≤ 0.33 and a power of $1 - \beta \geq 0.8$.

6.4 Cell culture

Embryonic neural precursors were obtained from day 14 (E14) BALB/c mouse embryos. Cells were plated at a density of 3.6 x $10^5/cm^2$ onto poly-D-lysine-coated (Sigma-Aldrich) 24-well plates in DMEM-F12 (Gibco-Life Technologies) added with B27 supplement, human β-FGF and EGF (10ng/mL). Cells were then transduced with a retroviral vector encoding for PDGF-B and DsRed. After 7 days, 2 x 10^4 cells were intracranially injected into adult BALB/c mice. Tumor cells were then obtained by dissociation of PDGF-B/DsRed-induced gliomas (HGG^{pdgf} cells) and cultured in DMEM-F12 added with B27 supplement, human β-FGF and EGF (10ng/mL) on Matrigel (1:200, BD Bioscience). Murine HGG^{pdgf} cells were then transfected with pcDNA3-hHER2 plasmid by Lipofectamine (Life technologies), selected for their resistance to neomycin G418 and sorted by FACS based on the receptor expression [79].

Splenocytes were obtained from mechanical dissociation in RPMI 1640 medium (Gibco-Life Technologies) and filtration through 40 mm filter. After removal of erythrocytes (Erythrocytes lysis buffer, NH_4 Cl 155mM, $KHCO_3$ 10mM, EDTA 0.1 mM), splenocytes were either co-cultured with tumor cells or endogenous mouse fibroblasts, plated for ELISpot assay or stained for Immunocytometric analyses.

Syngeneic primary mouse fibroblasts were isolated from adult mouse ears. Tissues from BALB/c NAIVE ears were cut into pieces and treated with collagenase 2000U/mL in Hanks' Balanced Salt Solution (HBSS, 24020-091, Gibco-Life Technologies) for 25 min at 37°C. After 2 washes with HBSS, the sample was treated with 0.25% trypsin for 20 min at 37°C. The cell suspension was filtered with a 40μm filter and the obtained fibroblasts were maintained in DMEM with 10% FBS (Gibco-Life Technologies).

Co-culture consisted of 2.3 x 10^5 splenocytes plus 4.5 x 10^4 $mHGG^{pdgf}$, $mHGG^{pdgf}$-hHER2 or 5 x 10^3 mouse fibroblasts plated in 96-well plates coated with Matrigel (1:200; BD Biosciences) in DMEM/F12 (Gibco-Life Technologies) added with B27 supplement (Gibco-Life Technologies), recombinant β-FGF (10 ng/ml; PeproTech) and EGF (10 ng/ml; PeproTech). Cells were harvest after 3 and 7 days and stained for flow cytometric analysis, luciferase analysis and ELISA assays. After 7 days, the supernatant was collected, separated from cells via centrifugation (600 x g for 5 min) and stored at -20°C.

Co-culture for splenocytes activation were conducted with the same medium as for the other co-culture plus the Mix Beads: 30U/mL IL-2, 10ng/mL IL-15 and a Dynabeads to cell ratio of 1:1 (Life technology). Fresh medium was added to cell cultures every 3-4 days.

6.5 Flow cytometry

To analyze proliferation, splenocytes were stained with CFDA-SE (V12883, Invitrogen). Freshly collected splenocytes were washed twice in RPMI 1640 medium (Gibco-Life Technologies) and stained with 5μM CFDA-SE for 15 minutes at 37°C. Cells were then washed and resuspended in RPMI 1640 medium (Gibco-Life Technologies) with 10% FBS (Gibco-Life Technologies) for 20 min at 37°C. To get the t0 fluorescence value, 2 x 10^5 stained cells were analyzed at the flow cytometer right after CFDA-SE staining. For the co-culture, 2.3 x 10^5 stained splenocytes were plated either alone, with 4.5 x 10^4 mHGG^{pdgf} or mHGG^{pdgf}-hHER2 or 5 x 10^3 mouse fibroblasts. Cells were harvested at t7 and stained with CD45-PE Antibody (1:5000, 103105, BioLegend) and CD8a-APC Antibody (1:500, 100711, BioLegend), CD45-PE Antibody (1:5000, 103105, BioLegend) and CD19-APC Antibody (1:1000; 115511 BioLegend) and CD45-PE Antibody (1:5000, 103105, BioLegend) and rat Anti-Mouse CD4 (1:800, 550280, BD Pharmingen). The binding of the primary anti-mouse CD4 antibody was revealed with a secondary antibody anti-rat CF 660R (1:400, 20390, Biotium).

The percentage of CFDA-SE$^-$ and CD45$^+$/CD8$^+$, CD45$^+$/CD19$^+$ or CD45$^+$/CD4$^+$ cells was calculated. The amount of proliferating cells (CFDA-SE$^-$) co-cultured with tumor cells was normalized on the percentage of proliferating cells co-cultured with syngeneic mouse fibroblasts.

For the detection of MHC-I expression by flow cytometry cells were harvested after 3 days of co-culture. Splenocytes co-coltured with mHGG^{pdgf} and mHGG^{pdgf}-hHER2 were stained in suspension with APC-conjugated anti-mouse CD45 antibody (1:800; 559864 BD Biosciences) and with mouse monoclonal antibody against MHC-I (1:100; 14-5999-81 Invitrogen). Binding of the primary antibody was revealed with secondary antibody anti-mouse 488 (1:400; 115-545-166 Jackson Immunoresearch Laboratories). Secondary antibody stained cells were used as negative control.

To detect splenocytes-induced cell death at t7, co-cultured cells were stained with APC-conjugated anti-mouse CD45 antibody (1:800; 559864 BD Biosciences) and PE/Cy7-conjugated anti-mouse CD140a (PDGFR-α) monoclonal antibody (1:1000, 25-1401-82 Invitrogen), exclusively and ubiquitously expressed on tumor cells. After the staining, 2 x 10^4 NIH/3T3 cells (PDGFRα$^-$) were added as internal normalizer. The percentage of PDGFRα$^+$/CD45$^-$ (mHGG^{pdgf} or mHGG^{pdgf}-hHER2) tumor cells was normalized on the percentage of PDGFRα$^-$/CD45$^-$ (3T3/NIH).

FlowJo software v10.8 was used for flow cytometry data analyses.

6.6 ELISA

ELISA assay was performed with the Mouse Granzyme B Uncoated ELISA Kit (Invitrogen, 88-8022) in accordance with manufacturer instructions.

A 96-well plate was coated with an anti-mouse Granzyme B antibody over night at 4°C. Supernatants collected by a 7-days culture of splenocytes in combination with mHGG^{pdgf}, mHGG^{pdgf}-hHER2 or mouse fibroblasts were added and incubated overnight at 4°C. Granzyme B standard was plated to build the standard curve. The day after, a biotin-conjugated anti-mouse Granzyme B antibody was added for 1h at RT, followed by a 30 min incubation with avidin-HRP. Tetramethylbenzidine (TBM)

Substrate Solution was added for 15 min and the color development was stopped with a Stop Solution (1M, H_3PO_4).
Plates were read at 450 nm and 570 nm with a BioTek plate reader (EL808 microplate reader, BioTek). Values of 570 nm were subtracted from those of 450 nm. Sample concentrations were determined with standard curve (range of 0-5000 pg/ml) after blank subtraction. The standard curve was built with a local polynomial regression in R.

6.7 ELISpot

ELISpot assay was performed using the Mouse IFNγ ELISpotBASIC kit (Mabtech, 3321-2A) in accordance with manufacturer instructions.
A 96-well plate was coated with a mouse monoclonal antibody against IFNγ and 2 x 10^5 freshly collected splenocytes were seeded and, after 48h, a detection antibody biotin-conjugated (mAb R4-6A2) was added to the wells for 2h, followed by 1h incubation with streptavidin conjugated with alkaline phosphatase (ALP). The chromogen substrate (BCIP/NBT-plus) was added until the spot revelation.

6.8 Luciferase assay

Luciferase enzyme can oxidize luciferin yielding to the production of a fluorescent product that can be quantified by measuring the release of light. For the luciferase assay, 1.15 x 10^6 splenocytes were incubated with 2.3 x 10^5 mHGG^{pdgf} cells expressing the firefly luciferase gene encoding for the corresponding enzyme (mHGG^{pdgf}-LUC). After 7 days of co-culture, cells were harvested, washed twice with PBS (Gibco-Life Technologies) and lysed with a lysis buffer (E195A, Promega). Then, the lysate was incubated with luciferin at a 1:4 ratio. The amount of light emitted was measured with a luminometer (GloMax 20/20, Promega) and represented as Relative Light Unit (RLU). Values were normalized on mHGG^{pdgf}-LUC cells that were not co-cultured with splenocytes.

6.9 Statistical analysis

Sample sizes for each experiment are indicated in the results. Statistical analyses were performed with two-sided t-test when between two conditions. Survival analyses were performed with log-rank test. Error bars represents standard deviation. Numeric values are reported as mean+/- standard deviation.

7 Discussion

Our previous experiments conducted on mice inoculated with mHGG^{pdgf}-hHER2 tumor cells and treated with the oncolytic HSV R-115, capable to target hHER2 and to produce murine IL-12, resulted into encouraging data [83]. For a closer translatability to the clinic, we decided to deeper investigate the efficacy of R-115 in a patient-like scenario. For this purpose, we evaluated the effect of R-115 treatment on an immunocompetent murine model of high-grade glioma originated from a mixture of cells (mHGG^{pdgf}-MIX) in which only a fraction of cells expressed hHER2 and was directly targetable by R-115. Exceeding the best expectations, we found that the treatment of mice inoculated with mHGG^{pdgf}-MIX had an outcome overlapping that of mice inoculated with mHGG^{pdgf}-hHER2: compared to controls, the overall survival was increased in both treated groups and the percentage of rescued mice was also similar.

To evaluate if we could further ameliorate the outcome of R-115 treated mice, we tested different treatment schedules which showed no differences between the arms. These results do not necessarily mean that there is no space for improvement by further tuning the administration schedules.

Our results showed a higher variability between the outcome of different treatment schedules in the mHGG^{pdgf}-MIX groups compared to the mHGG^{pdgf}-hHER2 ones. This could reflect possible unbalance between the two cell-fractions of a mixed population (hHER2-positive and hHER2-negative) arising during tumor growth under oHSV-killing pressure.

Another important outcome was that R-115 immunovirotherapy allowed to establish a solid immune response in surviving mice which were capable to eradicate secondary transplanted tumors (even hHER2-negative). The characterization of the status of the immune system of the rescued mice showed that splenocytes from long surviving mice were actively responding to tumor cells with an enhanced production of IFNγ and increased CD8, CD19 and CD4 cells proliferation. When co-cultured with tumor cells, splenocytes from long survivors were also capable to restore MHC-I expression which is known to be downmodulated by tumor cells as a strategy to be less recognizable by the immune system. The splenocytes antitumor effect was also directly measurable in terms of tumor cells reduction in co-culture.

The increased survival obtained by treating mHGG^{pdgf} bearing mice with ex vivo activated splenocytes from LS mice further consolidates the central role of the immune system in the complex reaction against high grade glioma and put the basis for further investigation where ex vivo activated splenocytes could be applied as a therapeutic strategy.

All together, these results underline that the role of R-115 for the treatment of glioblastoma was not only the direct targeting of hHER2 expressing cells but also the induction of an immune response capable to change a cold tumor like glioblastoma into a hot one, thus prolonging survival and rescuing almost one third of treated mice. The immune response developed thanks to R-115 treatment was so strong and long lasting that it was capable to prevent the engrafting and tumor growth when rechallenged.

Finally, in our model, we treated mice with intratumor injection without previous tumor resection, while in a clinical approach, patients would most likely undergo surgery and receive R-115 as an

integrative post operative treatment, with the aim to eradicate the tumor cells left and to prevent relapses.

8 Conclusion

Oncolytic virotherapy has already showed its efficacy for the treatment of tumors like metastatic melanoma, where T-VEC was the first oncolytic virus approved. Many OVs are currently under investigation and reached clinical trials but, in accordance with the engineered virus employed, there are still limits, often associated with viral spread or limited efficacy. Our results strongly highlight how R-115, remodeled for the expression of human IL-12, may represent a potential new therapy for the treatment of high-grade glioma.

References:

[1] T. Komori, «The 2021 WHO classification of tumors, 5th edition, central nervous system tumors: the 10 basic principles», *Brain Tumor Pathol*, vol. 39, fasc. 2, pp. 47–50, apr. 2022, doi: 10.1007/s10014-022-00428-3.

[2] D. N. Louis *et al.*, «The 2021 WHO Classification of Tumors of the Central Nervous System: a summary», *Neuro Oncol*, vol. 23, fasc. 8, pp. 1231–1251, giu. 2021, doi: 10.1093/neuonc/noab106.

[3] S. Gritsch, T. T. Batchelor, e L. N. Gonzalez Castro, «Diagnostic, therapeutic, and prognostic implications of the 2021 World Health Organization classification of tumors of the central nervous system», *Cancer*, vol. 128, fasc. 1, pp. 47–58, gen. 2022, doi: 10.1002/cncr.33918.

[4] J. R. McFaline-Figueroa e E. Q. Lee, «Brain Tumors», *The American Journal of Medicine*, vol. 131, fasc. 8, pp. 874–882, ago. 2018, doi: 10.1016/j.amjmed.2017.12.039.

[5] F. G. Davis, T. R. Smith, H. R. Gittleman, Q. T. Ostrom, C. Kruchko, e J. S. Barnholtz-Sloan, «Glioblastoma incidence rate trends in Canada and the United States compared with England, 1995–2015», *Neuro Oncol*, vol. 22, fasc. 2, pp. 301–302, feb. 2020, doi: 10.1093/neuonc/noz203.

[6] Q. T. Ostrom, H. Gittleman, G. Truitt, A. Boscia, C. Kruchko, e J. S. Barnholtz-Sloan, «CBTRUS Statistical Report: Primary Brain and Other Central Nervous System Tumors Diagnosed in the United States in 2011-2015», *Neuro Oncol*, vol. 20, fasc. suppl_4, pp. iv1–iv86, ott. 2018, doi: 10.1093/neuonc/noy131.

[7] C. Luo *et al.*, «The prognosis of glioblastoma: a large, multifactorial study», *Br J Neurosurg*, vol. 35, fasc. 5, pp. 555–561, ott. 2021, doi: 10.1080/02688697.2021.1907306.

[8] S. Larjavaara *et al.*, «Incidence of gliomas by anatomic location», *Neuro Oncol*, vol. 9, fasc. 3, pp. 319–325, lug. 2007, doi: 10.1215/15228517-2007-016.

[9] K. K. Das e R. Kumar, «Pediatric Glioblastoma», in *Glioblastoma*, S. De Vleeschouwer, A c. di Brisbane (AU): Codon Publications, 2017. Consultato: 24 ottobre 2022. [Online]. Disponibile su: http://www.ncbi.nlm.nih.gov/books/NBK469983/

[10] Y. T. Udaka e R. J. Packer, «Pediatric Brain Tumors», *Neurol Clin*, vol. 36, fasc. 3, pp. 533–556, ago. 2018, doi: 10.1016/j.ncl.2018.04.009.

[11] C. McKinnon, M. Nandhabalan, S. A. Murray, e P. Plaha, «Glioblastoma: clinical presentation, diagnosis, and management», *BMJ*, vol. 374, p. n1560, lug. 2021, doi: 10.1136/bmj.n1560.

[12] W. Stummer e E. Suero Molina, «Fluorescence Imaging/Agents in Tumor Resection», *Neurosurg Clin N Am*, vol. 28, fasc. 4, pp. 569–583, ott. 2017, doi: 10.1016/j.nec.2017.05.009.

[13] M. J. Colditz, K. van Leyen, e R. L. Jeffree, «Aminolevulinic acid (ALA)-protoporphyrin IX fluorescence guided tumour resection. Part 2: theoretical, biochemical and practical aspects», *J Clin Neurosci*, vol. 19, fasc. 12, pp. 1611–1616, dic. 2012, doi: 10.1016/j.jocn.2012.03.013.

[14] O. K. Dilmen, E. F. Akcil, A. Oguz, H. Vehid, e Y. Tunali, «Comparison of Conscious Sedation and Asleep-Awake-Asleep Techniques for Awake Craniotomy», *Journal of Clinical Neuroscience*, vol. 35, pp. 30–34, gen. 2017, doi: 10.1016/j.jocn.2016.10.007.

[15] T. Chowdhury *et al.*, «Anesthesia for Awake Craniotomy for Brain Tumors in an Intraoperative MRI Suite: Challenges and Evidence», *Front Oncol*, vol. 8, p. 519, nov. 2018, doi: 10.3389/fonc.2018.00519.

[16] G. Frosina, «Radiotherapy of High-Grade Gliomas: First Half of 2021 Update with Special Reference to Radiosensitization Studies», *Int J Mol Sci*, vol. 22, fasc. 16, p. 8942, ago. 2021, doi: 10.3390/ijms22168942.

[17] K.-C. Yoo *et al.*, «Proinvasive extracellular matrix remodeling in tumor microenvironment in response to radiation», *Oncogene*, vol. 37, fasc. 24, pp. 3317–3328, giu. 2018, doi: 10.1038/s41388-018-0199-y.

[18] A. Karachi, F. Dastmalchi, D. A. Mitchell, e M. Rahman, «Temozolomide for immunomodulation in the treatment of glioblastoma», *Neuro Oncol*, vol. 20, fasc. 12, pp. 1566–1572, nov. 2018, doi: 10.1093/neuonc/noy072.

[19] S. Yamamuro *et al.*, «Lomustine and nimustine exert efficient antitumor effects against glioblastoma models with acquired temozolomide resistance», *Cancer Sci*, vol. 112, fasc. 11, pp. 4736–4747, nov. 2021, doi: 10.1111/cas.15141.

[20] O. Rominiyi, A. Vanderlinden, S. J. Clenton, C. Bridgewater, Y. Al-Tamimi, e S. J. Collis, «Tumour treating fields therapy for glioblastoma: current advances and future directions», *Br J Cancer*, vol. 124, fasc. 4, pp. 697–709, feb. 2021, doi: 10.1038/s41416-020-01136-5.

[21] M. Abbott e Y. Ustoyev, «Cancer and the Immune System: The History and Background of Immunotherapy», *Semin Oncol Nurs*, vol. 35, fasc. 5, p. 150923, ott. 2019, doi: 10.1016/j.soncn.2019.08.002.

[22] G. P. Dunn, A. T. Bruce, H. Ikeda, L. J. Old, e R. D. Schreiber, «Cancer immunoediting: from immunosurveillance to tumor escape», *Nat Immunol*, vol. 3, fasc. 11, Art. fasc. 11, nov. 2002, doi: 10.1038/ni1102-991.

[23] F. Balkwill e A. Mantovani, «Inflammation and cancer: back to Virchow?», *The Lancet*, vol. 357, fasc. 9255, pp. 539–545, feb. 2001, doi: 10.1016/S0140-6736(00)04046-0.

[24] Q. Duan, H. Zhang, J. Zheng, e L. Zhang, «Turning Cold into Hot: Firing up the Tumor Microenvironment», *Trends in Cancer*, vol. 6, fasc. 7, pp. 605–618, lug. 2020, doi: 10.1016/j.trecan.2020.02.022.

[25] D. S. Chen e I. Mellman, «Elements of cancer immunity and the cancer–immune set point», *Nature*, vol. 541, fasc. 7637, pp. 321–330, gen. 2017, doi: 10.1038/nature21349.

[26] V. Thorsson *et al.*, «The Immune Landscape of Cancer», *Immunity*, vol. 48, fasc. 4, pp. 812-830.e14, apr. 2018, doi: 10.1016/j.immuni.2018.03.023.

[27] J. Zhang, D. Huang, P. E. Saw, e E. Song, «Turning cold tumors hot: from molecular mechanisms to clinical applications», *Trends in Immunology*, vol. 43, fasc. 7, pp. 523–545, lug. 2022, doi: 10.1016/j.it.2022.04.010.

[28] T. Bald, M. F. Krummel, M. J. Smyth, e K. C. Barry, «The NK cell–cancer cycle: advances and new challenges in NK cell–based immunotherapies», *Nat Immunol*, vol. 21, fasc. 8, Art. fasc. 8, ago. 2020, doi: 10.1038/s41590-020-0728-z.

[29] A. Addeo, A. Friedlaender, G. L. Banna, e G. J. Weiss, «TMB or not TMB as a biomarker: That is the question», *Crit Rev Oncol Hematol*, vol. 163, p. 103374, lug. 2021, doi: 10.1016/j.critrevonc.2021.103374.

[30] Y. Zhang e Z. Zhang, «The history and advances in cancer immunotherapy: understanding the characteristics of tumor-infiltrating immune cells and their therapeutic implications», *Cell Mol Immunol*, vol. 17, fasc. 8, pp. 807–821, ago. 2020, doi: 10.1038/s41423-020-0488-6.

[31] B. Mastelic-Gavillet, K. Balint, C. Boudousquie, P. O. Gannon, e L. E. Kandalaft, «Personalized Dendritic Cell Vaccines-Recent Breakthroughs and Encouraging Clinical Results», *Front Immunol*, vol. 10, p. 766, 2019, doi: 10.3389/fimmu.2019.00766.

[32] G. Dranoff *et al.*, «Vaccination with irradiated tumor cells engineered to secrete murine granulocyte-macrophage colony-stimulating factor stimulates potent, specific, and long-lasting anti-tumor immunity», *Proc Natl Acad Sci U S A*, vol. 90, fasc. 8, pp. 3539–3543, apr. 1993, doi: 10.1073/pnas.90.8.3539.

[33] S. A. Rosenberg, J. J. Mulé, P. J. Spiess, C. M. Reichert, e S. L. Schwarz, «Regression of established pulmonary metastases and subcutaneous tumor mediated by the systemic administration of high-dose recombinant interleukin 2», *J Exp Med*, vol. 161, fasc. 5, pp. 1169–1188, mag. 1985, doi: 10.1084/jem.161.5.1169.

[34] L. Zitvogel, L. Galluzzi, O. Kepp, M. J. Smyth, e G. Kroemer, «Type I interferons in anticancer immunity», *Nat Rev Immunol*, vol. 15, fasc. 7, pp. 405–414, lug. 2015, doi: 10.1038/nri3845.

[35] Q. Zhao *et al.*, «Engineered TCR-T Cell Immunotherapy in Anticancer Precision Medicine: Pros and Cons», *Front Immunol*, vol. 12, p. 658753, 2021, doi: 10.3389/fimmu.2021.658753.

[36] Y. Iwai, M. Ishida, Y. Tanaka, T. Okazaki, T. Honjo, e N. Minato, «Involvement of PD-L1 on tumor cells in the escape from host immune system and tumor immunotherapy by PD-L1 blockade», *Proc Natl Acad Sci U S A*, vol. 99, fasc. 19, pp. 12293–12297, set. 2002, doi: 10.1073/pnas.192461099.

[37] H. Ledford, «Melanoma drug wins US approval», *Nature*, vol. 471, fasc. 7340, p. 561, mar. 2011, doi: 10.1038/471561a.

[38] Q. Wu, L. Jiang, S. Li, Q. He, B. Yang, e J. Cao, «Small molecule inhibitors targeting the PD-1/PD-L1 signaling pathway», *Acta Pharmacol Sin*, vol. 42, fasc. 1, pp. 1–9, gen. 2021, doi: 10.1038/s41401-020-0366-x.

[39] O. L. Chinot *et al.*, «Bevacizumab plus Radiotherapy–Temozolomide for Newly Diagnosed Glioblastoma», *N Engl J Med*, vol. 370, fasc. 8, pp. 709–722, feb. 2014, doi: 10.1056/NEJMoa1308345.

[40] J. Litak, M. Mazurek, C. Grochowski, P. Kamieniak, e J. Roliński, «PD-L1/PD-1 Axis in Glioblastoma Multiforme», *Int J Mol Sci*, vol. 20, fasc. 21, p. 5347, ott. 2019, doi: 10.3390/ijms20215347.

[41] N. Zhang, L. Wei, M. Ye, C. Kang, e H. You, «Treatment Progress of Immune Checkpoint Blockade Therapy for Glioblastoma», *Frontiers in Immunology*, vol. 11, 2020, Consultato: 2 settembre 2022. [Online]. Disponibile su: https://www.frontiersin.org/articles/10.3389/fimmu.2020.592612

[42] A. A. Elsamadicy *et al.*, «Prospect of rindopepimut in the treatment of glioblastoma», *Expert Opin Biol Ther*, vol. 17, fasc. 4, pp. 507–513, apr. 2017, doi: 10.1080/14712598.2017.1299705.

[43] E. Khansur, A. H. Shah, K. Lacy, e R. J. Komotar, «Novel Immunotherapeutics for Treatment of Glioblastoma: The Last Decade of Research», *Cancer Invest*, vol. 37, fasc. 1, pp. 1–7, 2019, doi: 10.1080/07357907.2018.1479414.

[44] «History of Oncolytic Viruses: Genesis to Genetic Engineering | Elsevier Enhanced Reader». https://reader.elsevier.com/reader/sd/pii/S1525001616313314?token=15DECE0CDFC51925B52DB877A1F5064DF54D425F854C4E12F1577F48D696B2667B51DCB2FBE01EF218BD2DCE20FEDAC8&originRegion=eu-west-1&originCreation=20220817085349 (consultato 17 agosto 2022).

[45] «THE INFLUENCE OF COMPLICATING DISEASES UPON LEUKAEMIA. - ProQuest». https://www.proquest.com/openview/eb5cb1ae1913ff84c02cc61afbbd8d5e/1?cbl=41361&pq-origsite=gscholar (consultato 17 agosto 2022).

[46] H. R. Bierman *et al.*, «Remissions in leukemia of childhood following acute infectious disease: staphylococcus and streptococcus, varicella, and feline panleukopenia», *Cancer*, vol. 6, fasc. 3, pp. 591–605, mag. 1953, doi: 10.1002/1097-0142(195305)6:3<591::aid-cncr2820060317>3.0.co;2-m.

[47] H. A. Hoster, R. P. Zanes, e E. Von Haam, «Studies in Hodgkin's syndrome; the association of viral hepatitis and Hodgkin's disease; a preliminary report», *Cancer Res*, vol. 9, fasc. 8, pp. 473–480, ago. 1949.

[48] T. Asada, «Treatment of human cancer with mumps virus», *Cancer*, vol. 34, fasc. 6, pp. 1907–1928, dic. 1974, doi: 10.1002/1097-0142(197412)34:6<1907::aid-cncr2820340609>3.0.co;2-4.

[49] A. E. Moore, «Viruses with Oncolytic Properties and Their Adaptation to Tumors», *Annals of the New York Academy of Sciences*, vol. 54, fasc. 6, pp. 945–952, 1952, doi: 10.1111/j.1749-6632.1952.tb39969.x.

[50] D. Watanabe e F. Goshima, «Oncolytic Virotherapy by HSV», in *Human Herpesviruses*, vol. 1045, Y. Kawaguchi, Y. Mori, e H. Kimura, A c. di Singapore: Springer Singapore, 2018, pp. 63–84. doi: 10.1007/978-981-10-7230-7_4.

[51] A. Rodríguez-Camacho *et al.*, «Glioblastoma Treatment: State-of-the-Art and Future Perspectives», *Int J Mol Sci*, vol. 23, fasc. 13, p. 7207, giu. 2022, doi: 10.3390/ijms23137207.

[52] S. Zhu e A. Viejo-Borbolla, «Pathogenesis and virulence of herpes simplex virus», *Virulence*, vol. 12, fasc. 1, pp. 2670–2702, doi: 10.1080/21505594.2021.1982373.

[53] S. A. Connolly, T. S. Jardetzky, e R. Longnecker, «The structural basis of herpesvirus entry», *Nat Rev Microbiol*, vol. 19, fasc. 2, pp. 110–121, feb. 2021, doi: 10.1038/s41579-020-00448-w.

[54] R. J. Diefenbach e C. Fraefel, A c. di, *Herpes simplex virus: methods and protocols*, Second edition. New York, NY: Humana Press, 2020.

[55] A. V. Nicola, «Herpesvirus entry into host cells mediated by endosomal low pH», *Traffic*, vol. 17, fasc. 9, pp. 965–975, set. 2016, doi: 10.1111/tra.12408.

[56] A. L. Cunningham *et al.*, «The Cycle of Human Herpes Simplex Virus Infection: Virus Transport and Immune Control», *J INFECT DIS*, vol. 194, fasc. s1, pp. S11–S18, set. 2006, doi: 10.1086/505359.

[57] D. J. McGeoch *et al.*, «The complete DNA sequence of the long unique region in the genome of herpes simplex virus type 1», *J Gen Virol*, vol. 69 (Pt 7), pp. 1531–1574, lug. 1988, doi: 10.1099/0022-1317-69-7-1531.

[58] Y. Nishiyama, «Herpesvirus genes: molecular basis of viral replication and pathogenicity», *Nagoya J Med Sci*, vol. 59, fasc. 3–4, pp. 107–119, dic. 1996.

[59] C. M. Menendez e D. J. J. Carr, «Defining Nervous System Susceptibility During Acute and Latent Herpes Simplex Virus-1 Infection», *J Neuroimmunol*, vol. 308, pp. 43–49, lug. 2017, doi: 10.1016/j.jneuroim.2017.02.020.

[60] T. A. Stavropoulos e C. A. Strathdee, «An Enhanced Packaging System for Helper-Dependent Herpes Simplex Virus Vectors», *J Virol*, vol. 72, fasc. 9, pp. 7137–7143, set. 1998, doi: 10.1128/JVI.72.9.7137-7143.1998.

[61] S. Warming, N. Costantino, D. L. Court, N. A. Jenkins, e N. G. Copeland, «Simple and highly efficient BAC recombineering using galK selection», *Nucleic Acids Res*, vol. 33, fasc. 4, p. e36, 2005, doi: 10.1093/nar/gni035.

[62] M. S. Koch, S. E. Lawler, e E. A. Chiocca, «HSV-1 Oncolytic Viruses from Bench to Bedside: An Overview of Current Clinical Trials», *Cancers (Basel)*, vol. 12, fasc. 12, p. 3514, nov. 2020, doi: 10.3390/cancers12123514.

[63] T. Mineta, S. D. Rabkin, T. Yazaki, W. D. Hunter, e R. L. Martuza, «Attenuated multi-mutated herpes simplex virus-1 for the treatment of malignant gliomas», *Nat Med*, vol. 1, fasc. 9, pp. 938–943, set. 1995, doi: 10.1038/nm0995-938.

[64] A. R. MacLean, M. Ul-Fareed, L. Robertson, J. Harland, e S. M. Brown, «Herpes simplex virus type 1 deletion variants 1714 and 1716 pinpoint neurovirulence-related sequences in Glasgow strain 17+ between immediate early gene 1 and the "a" sequence», *Journal of General Virology*, vol. 72, fasc. 3, pp. 631–639, mar. 1991, doi: 10.1099/0022-1317-72-3-631.

[65] S. M. Brown, J. Harland, A. R. MacLean, J. Podlech, e J. B. Clements, «Cell type and cell state determine differential in vitro growth of non-neurovirulent ICP34.5-negative herpes simplex virus types 1 and 2», *Journal of General Virology*, vol. 75, fasc. 9, pp. 2367–2377, set. 1994, doi: 10.1099/0022-1317-75-9-2367.

[66] H. Kambara, H. Okano, E. A. Chiocca, e Y. Saeki, «An Oncolytic HSV-1 Mutant Expressing ICP34.5 under Control of a Nestin Promoter Increases Survival of Animals even when Symptomatic from a Brain Tumor», *Cancer Research*, vol. 65, fasc. 7, pp. 2832–2839, apr. 2005, doi: 10.1158/0008-5472.CAN-04-3227.

[67] K. A. Cassady, «Human Cytomegalovirus TRS1 and IRS1 Gene Products Block the Double-Stranded-RNA-Activated Host Protein Shutoff Response Induced by Herpes Simplex Virus Type 1 Infection», *Journal of Virology*, vol. 79, fasc. 14, pp. 8707–8715, lug. 2005, doi: 10.1128/JVI.79.14.8707-8715.2005.

[68] T. Todo, R. L. Martuza, S. D. Rabkin, e P. A. Johnson, «Oncolytic herpes simplex virus vector with enhanced MHC class I presentation and tumor cell killing», *Proc Natl Acad Sci U S A*, vol. 98, fasc. 11, pp. 6396–6401, mag. 2001, doi: 10.1073/pnas.101136398.

[69] J. M. Markert *et al.*, «Conditionally replicating herpes simplex virus mutant, G207 for the treatment of malignant glioma: results of a phase I trial», *Gene Ther*, vol. 7, fasc. 10, pp. 867–874, mag. 2000, doi: 10.1038/sj.gt.3301205.

[70] J. M. Markert *et al.*, «Phase Ib Trial of Mutant Herpes Simplex Virus G207 Inoculated Pre-and Post-tumor Resection for Recurrent GBM», *Mol Ther*, vol. 17, fasc. 1, pp. 199–207, gen. 2009, doi: 10.1038/mt.2008.228.

[71] J. M. Markert *et al.*, «A Phase 1 Trial of Oncolytic HSV-1, G207, Given in Combination With Radiation for Recurrent GBM Demonstrates Safety and Radiographic Responses», *Mol Ther*, vol. 22, fasc. 5, pp. 1048–1055, mag. 2014, doi: 10.1038/mt.2014.22.

[72] R. Rampling *et al.*, «Toxicity evaluation of replication-competent herpes simplex virus (ICP 34.5 null mutant 1716) in patients with recurrent malignant glioma», *Gene Ther*, vol. 7, fasc. 10, Art. fasc. 10, mag. 2000, doi: 10.1038/sj.gt.3301184.

[73] V. Papanastassiou *et al.*, «The potential for efficacy of the modified (ICP 34.5(-)) herpes simplex virus HSV1716 following intratumoural injection into human malignant glioma: a proof of principle study», *Gene Ther*, vol. 9, fasc. 6, pp. 398–406, mar. 2002, doi: 10.1038/sj.gt.3301664.

[74] S. Harrow *et al.*, «HSV1716 injection into the brain adjacent to tumour following surgical resection of high-grade glioma: safety data and long-term survival», *Gene Ther*, vol. 11, fasc. 22, pp. 1648–1658, nov. 2004, doi: 10.1038/sj.gt.3302289.

[75] D. M. Patel, P. M. Foreman, L. B. Nabors, K. O. Riley, G. Y. Gillespie, e J. M. Markert, «Design of a Phase I Clinical Trial to Evaluate M032, a Genetically Engineered HSV-1 Expressing IL-12, in Patients with Recurrent/Progressive Glioblastoma Multiforme, Anaplastic Astrocytoma, or Gliosarcoma», *Hum Gene Ther Clin Dev*, vol. 27, fasc. 2, pp. 69–78, giu. 2016, doi: 10.1089/humc.2016.031.

[76] T. Todo, Y. Ino, H. Ohtsu, J. Shibahara, e M. Tanaka, «A phase I/II study of triple-mutated oncolytic herpes virus G47Δ in patients with progressive glioblastoma», *Nat Commun*, vol. 13, p. 4119, lug. 2022, doi: 10.1038/s41467-022-31262-y.

[77] T. Todo *et al.*, «Intratumoral oncolytic herpes virus G47Δ for residual or recurrent glioblastoma: a phase 2 trial», *Nat Med*, vol. 28, fasc. 8, pp. 1630–1639, 2022, doi: 10.1038/s41591-022-01897-x.

[78] C. Dai, J. C. Celestino, Y. Okada, D. N. Louis, G. N. Fuller, e E. C. Holland, «PDGF autocrine stimulation dedifferentiates cultured astrocytes and induces oligodendrogliomas and oligoastrocytomas from neural progenitors and astrocytes in vivo», *Genes Dev*, vol. 15, fasc. 15, pp. 1913–1925, ago. 2001, doi: 10.1101/gad.903001.

[79] E. Reisoli *et al.*, «Efficacy of HER2 retargeted herpes simplex virus as therapy for high-grade glioma in immunocompetent mice», *Cancer Gene Ther.*, vol. 19, fasc. 11, pp. 788–795, nov. 2012, doi: 10.1038/cgt.2012.62.

[80] W. P. Halford, J. W. Balliet, e B. M. Gebhardt, «Re-evaluating natural resistance to herpes simplex virus type 1», *J Virol*, vol. 78, fasc. 18, pp. 10086–10095, set. 2004, doi: 10.1128/JVI.78.18.10086-10095.2004.

[81] E. Gambini *et al.*, «Replication-competent Herpes Simplex Virus Retargeted to HER2 as Therapy for High-grade Glioma», *Molecular Therapy*, vol. 20, fasc. 5, pp. 994–1001, mag. 2012, doi: 10.1038/mt.2012.22.

[82] E. K. Hellums *et al.*, «Increased efficacy of an interleukin-12-secreting herpes simplex virus in a syngeneic intracranial murine glioma model», *Neuro Oncol*, vol. 7, fasc. 3, pp. 213–224, lug. 2005, doi: 10.1215/S1152851705000074.

[83] F. Alessandrini *et al.*, «Eradication of glioblastoma by immuno-virotherapy with a retargeted oncolytic HSV in a preclinical model», *Oncogene*, vol. 38, fasc. 23, pp. 4467–4479, giu. 2019, doi: 10.1038/s41388-019-0737-2.

[84] F. Alessandrini *et al.*, «Eradication of glioblastoma by immuno-virotherapy with a retargeted oncolytic HSV in a preclinical model», *Oncogene*, vol. 38, fasc. 23, pp. 4467–4479, 2019, doi: 10.1038/s41388-019-0737-2.

[85] F. Castro, A. P. Cardoso, R. M. Gonçalves, K. Serre, e M. J. Oliveira, «Interferon-Gamma at the Crossroads of Tumor Immune Surveillance or Evasion», *Front Immunol*, vol. 9, p. 847, mag. 2018, doi: 10.3389/fimmu.2018.00847.

[86] A. Kane e I. Yang, «Interferon-gamma in Brain Tumor Immunotherapy», *Neurosurgery Clinics of North America*, vol. 21, fasc. 1, pp. 77–86, gen. 2010, doi: 10.1016/j.nec.2009.08.011.

[87] I. Voskoboinik, J. C. Whisstock, e J. A. Trapani, «Perforin and granzymes: function, dysfunction and human pathology», *Nat Rev Immunol*, vol. 15, fasc. 6, pp. 388–400, giu. 2015, doi: 10.1038/nri3839.